Macrophage epigenetic memories of early life injury drive neonatal nociceptive priming.

Adam J. Dourson[1], Adewale O. Fadaka[1], Anna M. Warshak[1], Aditi Paranjpe[2], Benjamin Weinhaus[3], Luis F. Queme[1], Megan C. Hofmann[1], Heather M. Evans[4], Omer A. Donmez[5], Carmy Forney[5], Matthew T. Weirauch[5,6,7], Leah C. Kottyan[5,6,8], Daniel Lucas[3,8], George S. Deepe, Jr.[9], Michael P. Jankowski[1,8,10*]

[1] Department of Anesthesia, Division of Pain Management, Cincinnati Children's Hospital Medical Center, [2] Biomedical Informatics, Cincinnati Children's Hospital Medical Center, [3] Division of Experimental Hematology and Cancer Biology, Cincinnati Children's Medical Center, [4] Division of Infectious Diseases, University of Cincinnati, [5] Center for Autoimmune Genomics and Etiology, Cincinnati Children's Hospital Medical Center, Cincinnati, Ohio, United States of America. [6] Division of Allergy and Immunology, Cincinnati Children's Hospital Medical Center, Cincinnati, Ohio, United States of America. [7] Divisions of Biomedical Informatics and Developmental Biology, Cincinnati Children's Hospital Medical Center. [8] Department of Pediatrics, University of Cincinnati, College of Medicine, Cincinnati, OH 45229. [9] Department of Medicine, Division of Infectious Diseases, University of Cincinnati College of Medicine, [10] Pediatric Pain Research Center, Cincinnati Children's Hospital Medical Center

***Corresponding author:**

Michael P. Jankowski
3333 Burnet Avenue, MLC6016
Cincinnati, Ohio 45229-3026
Telephone: (513) 803-7966
E-mail: michael.jankowski@cchmc.org

Conflict of interest:

The authors declare no competing financial interests.

Abstract

The developing peripheral nervous and immune systems are functionally distinct from adults. These systems are vulnerable to effects of early life injury which can influence outcomes related to nociception following subsequent injury later in life (i.e. “neonatal nociceptive priming”). The underpinnings of this phenomenon are largely unknown, although macrophages can be epigenetically trained by injury. We found that macrophages are both necessary and partially sufficient to drive neonatal nociceptive priming possibly due to a long-lasting epigenetic remodeling of peripheral macrophages. The p75 neurotrophic factor receptor (NTR) was observed to be an important effector in regulating neonatal nociceptive priming. p75NTR modulates the inflammatory profile and responses of rodent and human macrophages. This “pain memory” was able to be transferred to a naive host to alter sex-specific pain-related behaviors. This study reveals a novel mechanism by which acute post-surgical pain may transition to chronic pain in children.

Introduction

Several biological systems are activated following a peripheral injury to evoke an appropriate motor and affective response to sensory stimuli. To generate and maintain nociceptive signals, there is remarkable crosstalk between cellular systems to create distinct molecular patterns that depend on the given aversive event[1,2]. Importantly, these systems undergo significant developmental changes especially in early life[3,4], a time period where nociceptors and immune cells display unique properties compared to their adult counterparts[5-10].

Critical periods are constrained time points of high plasticity in which typical development can be permanently altered by external input. Clinical studies indicate that early life surgery or time

spent in the neonatal intensive care unit (NICU) alters the development of the somatosensory system[11,12]. In these patients, injury in adulthood has a higher risk of complications including increased pain medication use and longer hospital stays. Rodent drug studies revealed that the peripheral drive is necessary for this phenomenon termed “neonatal nociceptive priming”[13]. However, the peripheral and developmental factors that influence this experience are not fully known.

Immune cells, particularly macrophages, are known to modulate nociceptive responses. Patient recovery from surgery correlates with their pre-operative inflammatory profile[14-20]. In rodents, the depletion or addition of macrophages alters pain-like behaviors indicating a key role for neuroimmune signaling in the nociceptive response[5,20-23]. Evidence also suggests that macrophages “learn” to respond differentially to multiple exposures of the same or similar adverse agents, likely through epigenetic remodeling[24-26]. However, long-term changes within macrophages after neonatal injury and the role of macrophage memory in nociceptive development have not been investigated.

Aversive stimuli within the first week of life alters sensory neuron development by modifying key signaling pathways, such as neurotrophic factors[6,7,27]. Similar effects may be present in immune cells after an injury, however, much less is understood[28,29]. p75NTR (also known as nerve growth factor receptor (NGFR)) modulates broad neurotrophic factor signaling pathways[30] resulting in differential transcriptional and functional effects on neurons[31] and immune cells[28]. It is therefore reasonable to suggest that neurotrophin signaling is critical for development of the nervous and immune systems and could play a dual role in both neonatal inflammation and pain.

Pediatric post-surgical pain is a major problem that is complicated by underlying differences in patients, diagnostic uncertainty, and developmental concerns[32-35]. There is often a choice between patients suffering the negative developmental effects of pain or the side effects of current treatments (NSAIDs, steroids, anticonvulsants, opioids, etc.[36,37]). Improved therapeutics designed for early life pain are necessary for precision care. Here, we aimed to investigate how early life injury alters the peripheral neuroimmune system to prime animals to adverse outcomes following re-injury later in life. We determined the necessity and sufficiency of macrophages for neonatal nociceptive priming and evaluated epigenetic changes that occur in macrophages after neonatal injury that may underlie this phenomenon. We hypothesized that injury-induced epigenetic changes to chromatin accessibility in developing macrophages contributes to neonatal nociceptive priming.

Results

Macrophages are necessary for nociceptive priming.

Previous data indicate that macrophages are important for acute nociception in adults and neonates[5,21,38]. To establish the role of neonatal macrophages in the maintenance of neonatal nociceptive priming, we used macrophage fas-induced apoptosis (MaFIA) animals to ablate macrophages early in life and tested animals before and after both neonatal and adolescent incision (Fig. 1A). We found that injection of the designer drug AP20187 (AP) drastically reduced splenic macrophages but not microglia in the spinal cord (Supp. Fig. 1A-B), as has been similarly noted in adults[39,40]. This knockout strategy also prevented macrophage infiltration into injured muscle one day after a neonatal incision (Fig. 1B). Both vehicle and AP treated groups displayed significant paw guarding one day after a neonatal incision, with no statistical difference between groups (Fig. 1C, *$p<0.001$ vs. baseline (BL), $p=0.071$ AP vs. vehicle). However, while vehicle treated animals displayed a reduction in mechanical withdrawal

thresholds to muscle squeezing one day after incision (*p=0.014 vs. BL), AP treated animals were hyposensitive compared to baseline and controls (Fig. 1D, *p=0.007 vs. BL, ^p=0.028 vs. vehicle).

We then allowed animals of the same groups to age to P35 when sensory neurons and immunological functions are more developed[6,7,41,42]. At this time point, we first performed evaluations to determine any long-lasting effects of early life incision. Prior to second incision at P35, we evaluated muscle integrity and macrophage presence (Supp. Fig. 1C). Evans Blue Dye (EBD), when administered peripherally, is unable to penetrate into myofiber bundles unless they are damaged or undergoing repair[43]. Two days post adolescent injury, we observed about half of the myofibers stained positive for EBD. However, we found significantly less EBD staining within myofibers in animals that received an early life injury or early life sham (Supp. Fig. 1D-E, *p<0.001 vs. 2d post inc.). There were very few macrophages still present in the muscle of monocyte/macrophage reporter animals (LysMtdTom) at P35 after neonatal sham or incision surgery (Supp. Fig. 1F, p=0.648 vs. n.sham).

To determine the effect of early life injury in the presence or absence of macrophages on re-injury pain-like behaviors, we evaluated MaFIA animals treated with AP or vehicle early in life that received either a P7 sham or incision surgery. At adolescent baseline, prior to second incision, we observed no differences between any groups for paw guarding or muscle squeezing. One day after P35 incision, we found expected acute pain-like behaviors from all groups. N.sham animals from both treatments returned to baseline levels of paw guarding after day three (Fig. 1E, *p<0.05 vs. BL for all groups) and muscle withdrawal thresholds after day seven (Fig. 1F, *p<0.001 vs. BL for all groups). We detected no effect of the early life macrophage knockout on nociceptive development in n.sham+AP animals (n.sham+vehicle vs. n.sham+AP). N.inc animals that received vehicle treatment early in life had long-lasting pain-like

behaviors to a second incision through day 14 for guarding (Fig. 1E, *p<0.001 vs. BL, ^p<0.05 vs. n.sham+vehicle, #p<0.001 vs. n.inc+AP) and day 21 for muscle squeezing (Fig. 1F, *p<0.001 vs. BL, ^p<0.005 vs. n.sham+vehicle, #p<0.005 vs. n.inc+AP). Early life ablation of macrophages rescued this persistent pain-like phenotype with animals displaying guarding and mechanical hypersensitivity only through day seven after second injury (Fig. 1E-F, guarding *p<0.05 vs. BL; squeezing *p<0.001 vs. BL). Animals of this group were not significantly different at any time point compared to the control n.sham+vehicle group.

To evaluate if the ablation of macrophages early in life alters the sensitization of sensory neurons following dual incision, we performed an *ex vivo* intact muscle/tibial-nerve/DRG/SC preparation (Fig. 2A). We evaluated multiple peripheral response properties seven days after the second incision in vehicle and AP treated mice where we saw a robust block of both spontaneous guarding and evoked muscle squeezing behaviors (see Figs. 1E-F). We found no difference in the conduction velocity (CV) of thinly myelinated group III afferents in animals treated with AP versus vehicle seven days after the second incision (Fig. 2B, p=0.987). However, unmyelinated group IV afferents showed a significant reduction in CV in AP treated animals versus vehicle treated animals (Fig. 2C, *p=0.048). After mechanical stimulation of receptive fields, we observed no change in mechanical force necessary to evoke an action potential (Fig. 2D, p=0.430).

Overall, we observed no difference in the firing dynamics on all neurons collectively (Supp. Fig. 2), but upon the analysis of subtypes, we found that chemosensitive and mechanically sensitive fibers (without cold responsiveness[44]), had a significant reduction in mechanical firing rate after incubation with noxious metabolites (Fig. 2E, *p=0.031). Neonatal vehicle injected animals do not show this difference after metabolite application. We further uncovered that vehicle treated nociceptors increased mechanical firing rates with increasing forces applied to the receptive

fields as has been previously reported[45]. However, early life AP treated animals lost this encoding capability (Fig. 2F). We found no differences in thermal or chemical firing rate or instantaneous frequencies between groups (Supp. Fig. 2). The proportion of responders in AP treated animals resulted in a significantly higher number of responders to mechanical stimuli (42% to 61%) with a corresponding, non-significant, reduction (43% to 27%) in the number of non-responder “silent” neurons (Fig. 2G, *p=0.049, #p=0.090). We observed no change in the proportion of polymodal neurons (Supp. Fig. 2). Together, these data indicate that the temporary loss of macrophages during neonatal injury, changes inherent sensory neuron dynamics as well as the encoding capability of these cells after a second injury later in life.

Adoptive transfer of “primed” macrophages drives increased mechanical hypersensitivity.

We next wanted to determine if macrophages isolated from neonatal incised animals were sufficient to evoke a "primed" response in older mice. To do this we performed adoptive transfer (AT) experiments in which the macrophages from one animal were isolated and transferred to a sex and age-matched host (Fig. 3A). The Csf1r driver in MaFIA animals also promotes GFP expression. These animals were thus used to isolate and sort peritoneal GFP+ cells (monocytes and macrophages) (Fig. 3B) which were then transferred to the right hindpaw of naïve hosts at P35. We first ensured that the AT was accepted by dissecting the site of injection as well as other immune-related tissues. We found GFP+ cells in WT hosts three weeks after the injection specifically at the muscle injection site and not in the nearby bone marrow, lymph node, nor spleen (Fig. 3C). After confirming the transfer, we then tested if n.sham or n.inc (primed) cells would alter the behavioral response of the host animal that was either left uninjured, or was concurrently incised. We determined that AT of n.sham-injected macrophages into an uninjured paw had no effect on paw guarding, but injection of primed cells induced low-level paw guarding that lasted for one day (Fig. 3D, *p=0.044 vs. BL). Injection of n.sham or primed cells in the

absence of injury also slightly reduced muscle squeezing thresholds, with no difference between groups (Fig. 3E, *p<0.05 D1, D3 vs. BL). However, if the AT was paired with a host P35 incision, we found that primed cells transferred into the injury environment increased mechanical hypersensitivity measured by muscle squeezing (Fig. 3E, ^p<0.01 D1, D3 vs. n.sham no incision). We observed no differential effect of primed cells on paw guarding with or without a host incision, indicating a modality-directed phenotype. These data indicate that an early life injury alters macrophages to recognize and differentially affect injury-related responses later in life.

Early life incision alters the peripheral macrophage epigenetic landscape.

To determine how immune cells might be altered by early life incision, we collected peritoneal monocytes/macrophages from three different conditions of reporter animals (LysMtdTom): P7 naïve; P35 naïve; and P7 incised, isolated at P35 (primed) (Fig. 4A). To test if early life injury altered the epigenetic landscape of macrophages, we performed an Assay for Transposase-Accessible Chromatin sequencing (ATAC-seq) to measure chromatin accessibility. Quality control confirmed our isolation and predicted that the sequenced cells were macrophages (Supp. Fig. 3). Principle component analysis (PCA) revealed distinct clustering of the three groups, indicating an overall effect of early life incision (Fig. 4B). We repeated these same conditions to evaluate gene expression using RNA-Seq, and found similar clustering in our bulk RNA-seq PCA (Fig. 4C). We evaluated the top 100 differentially accessible chromatin sites (Fig. 4D) and top 100 differentially expressed genes (DEG) (Fig. 4E) from age-matched macrophages that were either naïve or primed. We obtained 10 candidate genes that were both differentially accessible and expressed because of early life incision (Fig. 4F). From this list, we verified that NGFR (aka. p75NTR) showed differential regulation in macrophages (Fig. 4G-H). p75NTR has long been of interest for nervous system development and nociception, and it has

roles in macrophage differentiation and function[28,31]. We therefore decided to test whether macrophage p75NTR could modulate neonatal nociceptive priming.

We next crossed the inducible LysMCreERT2 animal with a p75NTR floxed animal[46]. Animals were first incised at P7. Beginning at P33 and continuing until P37, animals were then injected with tamoxifen to eliminate p75NTR from LysM+ cells. At P35, all animals received a second incision. Behavior was evaluated prior to and for three weeks following the P35 incision (Fig. 5A). To first verify our injection protocol, we obtained samples following the final injection of tamoxifen at P37. We found an overall decrease of p75NTR mRNA from total peritoneal isolated cells in knockout animals compared to controls (-43±51% LysMCreERT2;p75fl/fl vs. controls). A P35 incision resulted in a number of F4/80+ monocytes/macrophages that infiltrated the injured tissue, of which 31% were positive for p75NTR in control genotypes (Fig. 5B). The knockout of p75NTR from LysM+ cells resulted in a significant reduction in co-stained F4/80+ macrophages (Fig. 5C, *$p<0.05$ vs. controls). Behaviorally, we observed that the knockout of p75NTR specifically in macrophages caused an accelerated restoration of paw guarding (Fig. 5D) and blunted the severity of the mechanical sensitivity compared to controls. LysMCreERT2;p75NTRfl/fl animals were significantly less hypersensitive one day following an injury (^$p=0.01$ vs. controls) and recovered earlier than controls (Fig. 5E). We also determined that hypersensitivity of the contralateral paw (Supp. Fig. 3, contralateral data from Fig. 1) was also inhibited by p75NTR knockout in LysM+ cells (Supp. Fig. 3). These data indicate that p75NTR has a partial but critical role in the macrophage-driven cellular memory that drives nociceptive priming.

Knockout of p75NTR in macrophages alters neuroimmune communication in mouse and in human iPSCs.

We then wanted to test if macrophage p75NTR modulated nociceptive priming through its role in inflammation. To do this, we first isolated bone marrow from naïve animals at P35, differentiated them into macrophages[47], and measured the cytokine release in response to different stimuli using cytokine arrays. We tested the effect of knocking down p75NTR using an siRNA strategy (example arrays Fig. 6A; siRNA transfection Supp. Fig. 4). We tested the effect of stimulation of two neutrophins, NGF and BDNF, which both bind to p75NTR in addition to TrkA and TrkB, respectively. We compared these to negative (vehicle) and positive controls (lipopolysaccharide and interferon gamma (LPS+ IFNγ)) controls (Fig. 6B; full data Supp. Fig. 4). In murine cells, the knockdown of p75NTR in macrophages alone (sip75+Vehicle (Veh)) affected both pro- and anti-inflammatory cytokines. If stimulated with LPS+IFNγ, the response was predominately pro-inflammatory. NGF did not appear to alter many proteins alone in control cultures (Supp. Fig. 4), however, NGF+p75NTR knockdown caused a significant down regulation of pro-inflammatory cytokine release and increased anti-inflammatory cytokine production (*$p<0.05$ vs. siCON+Veh, ^$p<0.05$ vs. sip75+LPS+IFNγ, #$p=0.05$ vs. sip75+Veh, ##$p>0.05$ vs siP75+Veh; Fig. 6C). Fewer changes were observed when BDNF or a combination of NGF and BDNF was used (Supp. Fig. 4). Together with our previous data, this may indicate that the epigenetic regulation of p75NTR in macrophages that are exposed to early life injury could promote pro-inflammatory/pro-nociceptive factor release and the targeting of this receptor can reverse this profile.

To test if these effects are conserved in human cells to influence sensory function, we then performed similar experiments with NGF and p75NTR KD in human iPSC-derived macrophages (Fig. 6D). We extracted the media of vehicle or NGF stimulated iPSC-derived macrophages that were treated with either control or p75 targeting siRNAs and applied it directly to human iPSC-derived sensory neurons (Fig. 6E) loaded with the calcium indicator Rhodamine-2 (Rhod-2; Fig. 6F). After 24h incubation, we discovered that, there was a decreased calcium response to ATP

in iPSC derived sensory neurons that were previously incubated with media from hBMDMs treated with sip75+NGF (Fig. 6G-H). No differences were found after treatment with capsaicin (Fig. 6I). Together with our previous data, this suggests that neuroimmune signaling in murine and human cells is impacted by p75 expression.

Transplant of neonatal "primed" bone marrow alters incision-related behaviors.

Trained immunity describes the concept of a long-lasting cellular memory that allows the immune system to display an enhanced responses to subsequent insults. To determine if the bone marrow was affected by early life injury, we again isolated mouse BMDMs at P35 from neonatal incised or sham controls. We found no difference in the total number of bone marrow cells isolated due to an incision (Supp. Fig. 4). We then stimulated these cultured macrophages with LPS+IFNγ as an artificial second "injury" (Fig. 7A). We observed that early life injury impacted these cells as they responded with a greater pro-inflammatory profile compared to n.sham controls (Fig. 7B, *$p<0.05$ vs. controls+vehicle, ^$p<0.05$ vs. controls+LPS+IFNγ). These results indicate that incision induces a long-lasting (at least 28 days) reprogramming of hematopoietic progenitors to generate macrophages that are primed to respond more potently to inflammation.

To test if hematopoietic stem cells (HSCs) retain a memory of the incision that then contributes to nociception, we performed a bone marrow transplant (BMT) experiment. To do this, we performed a neonatal sham or incision (primed), allowed the animals to age until P35 and then performed a BMT into naive adolescent mice (Fig. 7C). After a 16-week recovery, when all hematopoietic cells are derived from the donated hematopoietic stem cells, animals were subjected to a hindpaw incision and were monitored for another 21 days. We successfully transferred the bone marrow evidenced by the vast majority of CD45.2+ donor cells and a

minority of CD45.1+ host cells (Fig. 7D). Prior to later in life incision, we detected an expected increase in p75NTR transcript from bulk isolated peritoneal cells (Fig. 7E). Further, we found that female peritoneal cells, regardless of condition, had 480 ± 25% more p75NTR than males ($p=0.016$, ANOVA on Ranks, Dunn's, n=4-5/sex). When we evaluated all animal behavior collectively following later in life incision, we uncovered little evidence of neonatal nociceptive priming in either group. Both groups displayed guarding behavior for only one day (Fig. 7F, *$p<0.001$ vs. BL) and mechanical hypersensitivity for several days (Fig. 7G, *$p<0.05$ vs. BL). However, we found an unexpected female-driven acceleration of mechanical sensitivity. Aged animals can show delayed onset pain-like behaviors[48] which we also detected in our control female animals but not in primed-cell recipient animals (Fig. 7H-I). One day after injury, female controls were not mechanically sensitive but female primed-cell recipient animals had a significant reduction from baseline (*$p=0.004$ vs. BL) and controls (^$p=0.006$ vs. controls). The length of injury-induced behaviors was not different between groups and there was no acceleration or delayed onset sensitivity in males (Fig. 7H-I). Together, these data describe an effect of early life incision on HSCs that can alter evoked pain-like behaviors and that this effect can be transferred to recipient mice after HSC transplantation.

Discussion

In this study, we uncovered a mechanism in which the peripheral immune system can form and maintain a "pain memory" following a neonatal hindpaw incision to modulate prolonged responses to repeated injury. Macrophages were found to be both necessary (Figs. 1-2) and partially sufficient (Fig. 3) to drive neonatal nociceptive priming responses at the behavioral and afferent levels. This single, local insult dramatically altered the systemic macrophage epigenetic/transcriptomic landscape (Fig. 4) and function through the p75NTR receptor in mouse and human cells (Figs. 5-6). The molecular effects of early life injury were also evident in BMDMs and following a BMT which induced a sex-specific alteration of injury related effects

(Fig. 7). This study is the first to show a macrophage cellular memory formed in neonates that modulates pain related outcomes. Together, these data help us to understand how the distinct cellular systems can be changed by an aversive event in early development to influence nociceptive processing across the lifespan.

Previous work has evaluated the vulnerable periods that exist in the somatosensory and immune systems[5,49-54] as well as genetic risk factors in children following surgery[32,55]. After neonatal injury, the inhibitory circuits and microglial activity of the spinal cord dorsal horn (SCDH) are dysregulated leading to hyperactivity of spinal output[56-60]. Moriarty et al found that a peripheral nerve block was sufficient to prevent neonatal nociceptive priming, while systemic morphine injection was not[13]. This highlights the importance of peripheral input to induce nociceptive priming and our work extends these findings to capture a neuroimmune mechanism.

Macrophages are one of the first immune cells at the injury site to promote inflammation and subsequent wound healing. This is accomplished through damage associated molecular patterns (DAMPs) which can be stimulated by, and also control, cytokine and growth factor responses. Both DAMPs and the effector proteins released may also be pro-nociceptive such as high-mobility group box 1 (HMGB1), IL1β and NGF[61-66]. ATP is another DAMP that is present in our metabolite mixture which we found to differentially alter the mechanical firing rate of chemosensitive neurons in animals that lacked macrophages during an early life incision (Fig. 2[62]). It may be that desensitization to a high metabolic/noxious tissue environment was a contributor to the rescuing of priming by early life macrophage ablation (Fig. 1). The conduction velocity slowing of group IV sensory neurons because of macrophage ablation was an intriguing finding. There are reports of activity dependent slowing of cutaneous unmyelinated fibers[67] but

this is unlikely to be the driving factor here because of the lack of spontaneous activity in these cells. There may be differences in the size of the population of neurons that could explain this phenomenon which could correlate with the differences in proportions of each type of fiber response detected (Fig. 2). AT experiments (Fig. 3) showed that macrophages are only partially sufficient to induce priming. This could suggest that other cells, including neurons, may contribute neonatal nociceptive priming. However, these concepts would need further investigation.

Neonatal macrophages are unique compared to the adult, with a distinct epigenetic landscape (Fig. 4) and differential responses to stimuli[14,49 9,10,24,68]. The macrophage epigenome is critical to differentiate monocytes to macrophages, and acute stimulation of these cells induces epigenetic modifications[69-71]. Changes in macrophages at the epigenetic level is one way in which these cells become either “trained” or “tolerant” to subsequent stimuli[25,26 54]. Recent work by Cobo et al reveals that infant nociceptive reflexes to noxious and non-noxious stimuli are altered by current or previous infection[72]. It is possible that an early life aversive event such as a surgical incision (or an infection) may generate molecular patterns that induce epigenetic priming in macrophages as was observed in the current study. Studies that interrupt neuroimmune signaling may prove beneficial for adverse injury-related effects such as pain as has been noted during infection[73-75]. It will be necessary to determine the factors that epigenetically train macrophages for future drug targeting.

While the initiating mechanism is yet unknown, we determined that p75NTR is one critical endpoint of the epigenetic modifications. In early development, neurotrophin signaling is necessary for sensory neuron specialization into distinct populations[76-79], which can be

modulated by p75NTR expression[31]. Macrophage p75NTR has been less studied, but HSCs express high levels of neutrophins, and we and others found that the inflammatory response from macrophages is directly affected by a loss of p75NTR (Fig. 6[29,80,81]). Developed immune cells regularly contain low levels of neurotropic factor receptors, but during inflammation they are robustly, and transiently, increased[5,28]. NGF in human derived macrophages modulates p75NTR expression and drives its co-localization with TrkA, which we found to have persistent upregulation in macrophages due to early life incision (data availability at NCBI: GSE224209)[81]. Further, Khodorova et al demonstrated that intraplantar NGF injections evoke expected pain-like behaviors, but that a general inhibition of the p75NTR receptor rescued the phenotype[82]. Combined with our data, this indicates that immune cell p75NTR increases their pro-inflammatory signature and that the ablation of this receptor can modulate pro-inflammatory signaling, blunt the ability of macrophages to communicate to sensory neurons, and partially prevent prolonged pain-like behaviors (Figs. 5-6).

Circulating immune cells that infiltrate injury sites are constantly replenished through the hematopoietic stem cell pool in the bone marrow. These are highly plastic cells that are differentially altered by injury type[83], infection[84] and development[28,85]. Our data support the notion that peripheral injury can alter these stem cells long-term, and changes in these cells are part of a system to maintain immune-related neonatal nociceptive priming (Figs. 4-7). The mechanism in which HSCs are notified of noxious stimuli is currently unknown, although there are potential avenues to be tested including direct immune or neuronal signaling[86], or indirect signals in the blood or cerebral spinal fluid[87]. Regardless, the results we find are reminiscent of trained immunity where an initial event is epigenetically retained in innate immune cells to enhance responses to subsequent activation[26]. In the context of immunity, the outcome is increased inflammation, while here the outcome was enhanced nociception. Evaluation of the

functional effects of injury on HSCs by BMT indicated a female-specific hastening of mechanical hypersensitivity. Interestingly, we detected no effect in spontaneous paw guarding between early life incised and control animals indicating a modality specific effect (Fig. 7). It may be that "primed" macrophages have direct signaling roles that involve mechanical sensation as we saw similar effects with AT (Fig. 3) and p75NTR knockout (Fig. 5) behaviors. An understanding of how stem cells may be changed by peripheral injury may have important clinical considerations for a number of conditions that impact childhood development.

There are multiple technical points to consider. The depletion of macrophages in MaFIA animals alters animal activity and, in some studies, withdrawal thresholds[38,88]. In our neonatal behavior, we detected no changes in baseline withdrawal reflexes nor guarding scores due to the knockout (Fig.1C-D). However, we did observe that when we directly manipulated macrophage presence, there was an impact on withdrawal reflexes, but not spontaneous behaviors (Figs. 1D, 3E, and our previous work[5]). Since withdrawal thresholds are one of the most utilized behavioral readouts, it may be prudent to consider multiple behavioral assays when performing experiments depleting macrophages[5,21,38,88,89]. This confound is not a major concern for adolescent/adult behaviors, however, because the animal's immune system had recovered before the second injury (Fig. 1E-F). Similar concerns are also avoided when performing adoptive transfer experiments because we tested latent changes in primed macrophages, a major strength of this study.

We considered sex as a critical factor throughout our study. In our RNA-seq, we noticed some indications of differences between the sexes, especially in the early life incised condition. We do not have the power to critically evaluate these against one another, however, there are multiple

lines of evidence that suggest the immune-modulated injury response differs between males and females[e.g.90]. In our BMT experiments, we observed a female-driven acceleration in injury-induced mechanical hypersensitivity after receiving primed cells (Fig. 7I). It is possible that this is due to the BMT or the age of the animal after recovery from the BMT (injury at 12-13 months old). Indeed, recently dos Santos et al found a delayed onset hypersensitivity in aged animals following an incision injury as well as blunted hyperalgesic priming in aged animals. This was connected with changes in inflammation in older rodents compared to younger animals[48]. Our data obviously includes a BMT which could impact the effect of age on incision injury. Nevertheless, results reveal that incisional "priming" of the bone marrow can be transferred to female animals which may accelerate nociceptive behaviors. Indeed, when evaluating the levels of p75NTR in our BMT animals, we found that isolated female peritoneal cells, had significantly more p75NTR than males (Results). These data, along with substantial literature on the heightened prevalence of chronic pain in females[91], warrant additional studies that examine sex differences in injury-induced changes in immune cells over time to help better understand these phenomena.

Clinical studies have shown that neonatal injuries can have the potential to cause a "primed" somatosensory system, and lead to long-term alterations in nociceptive processing[11,12,92,93]. The potential therapeutic ability of p75NTR inhibitors has been recently reviewed by Malik et al indicating a range of functional neurological disorders that are affected by p75NTR, while Norman and McDermott review potential therapeutic strategies in blocking p75NTR signaling for chronic pain[94,95]. New technologies that allow for the specific targeting of macrophage p75NTR could provide the specificity to prevent the priming effect of this receptor system[96]. Here, we discovered a change in the epigenetic landscape of macrophages due to early life incision that

modulated neonatal nociceptive priming. Future studies designed to analyze the immune “pain memory” may lead to important therapeutic interventions for pediatric post-surgical pain.

Author contributions:

A.J.D. and M.P.J. conceived and designed the study and wrote the manuscript. A.J.D. completed most of the experiments and collected most of the data. A.J.D. performed the analyses with input from M.P.J. A.F. completed the BMT behaviors and the human culture experiments. A.M.W. completed various experiments including some IHC and qPCR. A.P. completed bioinformatics data processing. L.F.Q. assisted in ex vivo recordings and interpretations of data. G. D. and H.E. facilitated experiments utilizing bone marrow isolation, differentiation and stimulation of macrophages. G.D. helped with the conceptualization of the study. D. L. and B.W. assisted with the BMT experiment planning and execution. O.D., C.F., M.T.W., and L.C.K. helped perform ATAC-Seq and RNA-Seq processing. M.C.H. managed the colony and performed genotyping assays.

Acknowledgements:

We would like to recognize others who have provided support for this project including: The Research Flow Cytometry Core in the Division of Rheumatology and the Confocal Imaging Core at CCHMC; Dr. Yoon at the Ohio State University who provided to us the p75NTRfl/fl animals; The Center for Autoimmune Genomics and Etiology (CAGE) at CCHMC and; The Comprehensive Mouse and Cancer Core for their assistance in the completion of the bone marrow transplants and care for the animals. This work was supported by grants from the NIH to M.P.J. (R01NS105715 and R01NS113965), A.J.D. (F31NS122494), D.L. (R01 HL160614),

L.C. K. (P30 AR070549), and a CCHMC ARC award (#53632) to L.C.K. and M.T.W.. D.L. is a scholar of the Leukemia and Lymphoma Society.

Figure Legends

Figure 1: Early life ablation of macrophage alters responses to re-injury later in life.

A. Schematic of the experimental design used in MaFIA mice. **B.** The treatment of MaFIA animals with AP early in life was sufficient to ablate macrophages at the injury site one day after the neonatal incision compared to vehicle treated controls. Scale bar, 10μM. **C.** Paw guarding one day after a neonatal incision with or without macrophage ablation indicated an effect of day (F=103.418) but no difference between groups (*p<0.001 vs. BL for AP and vehicle treated animals; p=0.071 AP treated vs. vehicle treated). **D.** Muscle squeezing in the same animals showed an interaction for withdrawal thresholds (F=16.647). Vehicle treated animals had a significant reduction from BL (*p=0.014 vs. BL) while incision+AP animals were hyposensitive (*p=0.007 vs. BL; groups were significantly different from one another at day one, ^p=0.028 vs. controls; two-way RM ANOVA; n=10-11/group). **E.** Animals that received an early life ablation of macrophages did not have altered baseline scores at adolescence, but the response to a second injury revealed a significant effect of dual incision (guarding F=5.635, muscle squeezing F=5.303). Groups that received a sham as neonates guarded through day 3 (*p<0.01 vs. BL) while vehicle treated dually incised animals guarded through day 14 (*p<0.001 vs. BL). Animals from the neonatal incision (n.inc)+AP group returned to BL guarding scores after seven days (*p<0.05 vs. BL). At days three, seven, and 14, the vehicle+incision group was significantly different compared to all other groups (^p<0.05 vehicle+incision vs. controls, #p<0.001 vs. incision+AP). **F.** In the same group of animals, a similar pattern was observed for muscle

squeezing withdrawal thresholds. N.sham operated groups were hypersensitive through day 7 (*p<0.005 vs. BL). The incision+vehicle group showed reduced thresholds through day 14 (*p<0.001 vs. BL), but incision+AP treated animals were hypersensitive only through day 3 (*p<0.001 vs. BL). At days three, seven and 14, the incision+vehicle group had significantly lower thresholds compared to all other groups (^p<0.005 vs controls, #p<0.005 vs. incision+AP). Colored horizontal lines indicate the duration of significance compared to BL for each group. Data shown as mean +/- SEM.

Figure 2. Macrophage depletion in neonates alters sensory neuron sensitization following repeated incision.

A. Representative image of the intact electrophysiological preparation containing the injured hindpaw muscle, tibial nerve, DRGs and SC. The search electrode (SE) and recording electrode (RE) are marked. **B.** There is no difference in CVs between groups in group III muscle afferents (p=0.987 n.AP vs. n.Vehicle, n=34 and 39 respectively, one way ANOVA, Tukey's) but (**C**) there is a significant reduction of group IV conduction velocities (H=3.896) in the neonatal treated AP group compared to vehicle (*p=0.048 n.AP vs. n.Vehicle, n=16 and 11 respectively, ANOVA on Ranks, Dunn's). **D.** There are no differences in overall mechanical thresholds between groups (p=0.430 n.AP vs. n.Vehicle, n=31 and 22 respectively, ANOVA on Ranks, Dunn's). **E.** There is no change in mechanical firing rate pre- to post- metabolite treatment in vehicle treatment group, unlike that seen in the AP treatment group (H=4.934, n.Vehicle: p=0.223, n.AP: *p=0.031, ANOVA on Ranks, Dunn's). **F.** There is a significant increase in firing rate over mechanical forces applied in the vehicle treatment (H=5.760) but not in the AP treatment group (n.Vehicle: *p=0.019, n.AP: p=0.149, ANOVA on Ranks, Dunn's). **G.** There is an increase in the number of mechanically sensitive cells in AP treated animals compared to vehicle treated animals (*p=0.049 n.AP vs. n.Vehicle, Chi-Square on mechanical responders), with a

corresponding non-significant decrease in cells that responded to no stimulus ("silent", #p=0.090 n.AP vs. n.Vehicle, Chi-Square on silent neurons). Data shown as mean +/- SEM.

Figure 3: Adoptive transfer of macrophages from neonatal incised animals increases pain-like behaviors.

A. Outline of the experiment design for AT experiments. **B.** Example of the sorting of live GFP+ peritoneal cells from MaFIA mice. **C.** Example images demonstrating the presence of GFP+ donated cells (arrows) in the hindpaw of a host 21 days after injection, but not in the bone marrow (ipsilateral tibia), lymph node (potineal), or spleen. Scale bars, 25μM; BM, 150μM. **D.** For guarding behaviors, there was an effect (F=3.132) of macrophage exposure to injury. Both primed and unprimed cells injected into an incision site induced prolonged guarding (*p<0.05 vs. BL). In the absence of injury at P35, primed cells induced one day of guarding (*p=0.044 vs. BL) while unprimed cells did not induce detectable behavior. There was a significant difference between primed+incision vs. n.sham without incision at days 1, 3 and 7 (^p<0.001 vs. n.sham) and between unprimed+incision vs. n.sham at days 1-14 (#p<0.05 vs. n.sham). **E.** The same animals were then tested for muscle withdrawal thresholds by muscle squeezing which resulted in a significant interaction (F=4.318). All groups had a significant reduction in withdrawal thresholds that varied over time depending on condition (*p<0.05 vs. BL). Primed+incision treatment was significantly different than n.sham alone animals at days 1 and 3 (^p<0.01 vs. n.sham). Unprimed vs. n.sham treatment showed an effect at day 14 (#p=0.015 vs. n.sham). Two-way RM ANOVA, Tukey's post hoc, n=8-11/group. Colored horizontal lines indicate the duration of significance compared to BL for each group. Data shown as mean +/- SEM.

Figure 4. Early life incision alters the epigenetic and mRNA landscape of LysM+ cells.

A. Example sorting of peritoneal macrophages from P7 naïve, P35 naïve, and P7 incised animals isolated at P35. **B.** Principle component analysis from ATAC-seq datasets demonstrating distinct clustering of groups. **C.** Principle component analysis form the RNA-seq dataset shows similar distinct clustering of groups. **D.** The top 100 differentially accessible chromatin regions in macrophages in P35 naïve cells compared to P35 primed cells (age matched). **E.** The top 100 differentially expressed genes (DEGs) for the same conditions. **F.** A table of factors that had differentially accessible regions and DEGs. NGFR (p75NTR) is highlighted. **G.** ATAC-Seq indicating higher reads of NGFR (*p=0.001 vs. controls, one-way ANOVA, Tukey's, n=3-4/group), and (**H**) transcripts per million (TPM) data for RNA-seq (*p=0.008 vs. controls). Data shown as mean +/- SEM.

Figure 5. Macrophage specific knockout of p75NTR after neonatal incision impacts neonatal nociceptive priming.

A. Schematic of knocking out p75NTR from macrophages following neonatal incision. **B.** Representative images of p75NTR labeling (green) co-stained with F4/80 (macrophages, white) in the injured hindpaw. Yellow arrows indicate double positive staining. Scale Bar, 25μM. **C.** There is a significant reduction (F=4.012) in the percentage of double positive cells in LysM;p75fl/fl animals compared to other genotypes (*p<0.05 vs. controls (p75+/fl and p75fl/fl) and LysM;p75+/fl, one way ANOVA, Tukey's, n=3-5/group). **D.** We found no effect of tamoxifen prior to the second injury (No Tam vs. BL time points) on paw guarding. Following the second incision there was robust paw guarding (F=26.258), with a faster recovery in the LysM;p75NTRfl/fl mice (**p<0.05 vs. BL, both groups, #p=0.05 vs BL). Two-way RM ANOVA, Tukey's. **E.** No effect of tamoxifen on mechanical withdrawal thresholds was found prior to injury (No Tam vs. BL time points), however there was an effect following a second incision (F=40.516). Both groups displayed mechanical sensitivity on days one, three and seven

(**p<0.01 vs. BL) but the p75fl/fl genotype continued to display significant sensitivities at day 14 while LysM;p75fl/fl animals did not (p75fl/fl: *p=0.002 vs. BL, LysM;p75fl/fl: p=0.063 vs. BL). At one day following second incision, LysM;p75fl/fl animals were less hypersensitive than controls (^p=0.01 vs. controls). Two-way RM ANOVA, Tukey's, n=7/group. Data shown as mean +/- SEM.

Figure 6. p75NTR expression in macrophages alters the inflammatory signature of macrophages and neuronal activity.

A. Examples of the protein arrays that were run on the lysates of BMDMs that received a knockdown of p75NTR and were stimulated with indicated factors. **B.** Heatmap indicating the protein expression detected across each stimulus, n=4/group. **C.** Examples of significantly regulated proteins detected from the protein array (*p<0.05 vs. siCON+Veh, ^p<0.05 vs. sip75+LPS, #p=0.05 vs. sip75+Veh, ##p>0.05 vs sip75+Veh; one-way ANOVA, Tukey's or ANOVA on Ranks, Dunn's. n=4/group). **D-F.** Representative images of iPSC-derived macrophages, sensory neurons and Rhod-2 responses to ATP. Arrows indicate increased responses. Arrowheads indicated new responses. **G.** Example calcium transients from iPSC derived sensory neurons in response to ATP or capsaicin stimulation. The arrow indicates when the ATP or capsaicin was added. Scale Bar, 20μM. **H.** Exposure of iPSC derived sensory neurons to media from macrophages with loss of p75NTR treated with NGF caused decreased responsiveness of neurons to ATP (F=4.257) (*p<0.04 vs. all other conditions, 1-way ANOVA with Tukey's post hoc, n=15 cells per group). **I**. No changes in calcium responses to capsaicin (F=2.702) were observed (1-way ANOVA). Data shown as mean +/- SEM or percent change from controls with variance.

Figure 7. Bone marrow transplant from neonatal incised animals transfers a "pain memory" to naïve animals.

A. A schematic indicating timeline for removal and stimulation of bone marrow cells from previously sham operated or incised neonates. **B.** Analyses of the transcripts from BMDMs after stimulation with LPS+IFNγ (*$p<0.05$ vs. n.sham no stimulation controls, ^$p<0.05$ vs. n.sham with stimulation, n=3-8/group, Two-way ANOVA, Tukey's). **C.** Schematic of the bone marrow transplant experiments. **D.** Representative cell sorting of living cells, 45.1+ host remaining cells and 45.2+ transferred cells. **E.** p75NTR transcripts are increased in animals that received an early life incision versus those that did not (total peritoneal cells). **F.** After recovery from the BMT, animals display no guarding behaviors prior to incision. Following an incision both n.sham and n.inc transferred groups display an effect of day ($F=25.051$) on paw guarding (*$p<0.001$ vs. BL, Two-way RM ANOVA, Tukey's). **G.** There was also an effect of day on withdrawal thresholds ($F=9.099$) that was significant at days one and three in the primed group (*$p<0.01$ vs. BL) but was delayed in controls with significant reductions at days three and seven (*$p<0.01$ vs. BL, Two-way RM ANOVA, Tukey's, n=10-11/group). **H.** There is no difference between groups for male-driven mechanical withdrawal thresholds but there is an effect of day ($F=6.867$) that was significant in controls (*$p<0.05$ vs. BL, Two-way RM ANOVA, Tukey's, n=6/group). **I.** In female mechanical withdrawal thresholds there was an interaction effect ($F=4.398$) with n.inc animals showing hypersensitivity at days one and three (*$p<0.05$ vs. BL) and controls at day seven (*$p=0.002$ vs. BL). At days one and seven, primed animals withdraw thresholds are significantly different compared to controls (^$p<0.05$ vs. controls, Two-way RM ANOVA, Tukey's, n=4-5/group). Data shown as mean +/- SEM.

Methods

Animals. Animals of both sexes were used for all studies. Neonatal animals were considered at postnatal day 7 (P7). Adolescent animals begun experimentation at P35-P42. Sex was analyzed as a critical biological factor for each experiment, and differences are noted in figure legends. In an effort to reduce stress, neonatal animals were kept with the dam when not actively analyzed behaviorally, and experiments were kept as short as possible (~1 hour, never more than 1.5 hours). In all behavioral experiments mice, were acclimated to the room and were performed by the same experimenter under the same conditions including time of day, location, lighting and temperature. Animals were used +/- 1 day from the indicated age. All animals were kept in an environment-controlled facility at Cincinnati Children's Hospital Medical Center with free access to food and water while on a 14/10-hour light/dark cycle.

C57/Bl6 (CD45.2^{+}) mice were bred in-house or purchased from Jax (Stock#: 000664). B6.SJL/BoyJ (CD45.1^{+}) mice were bred in the CCHMC transplant core. Macrophage fas-induced apoptosis (MaFIA) animals were purchased from Jax (Stock#: 005070) and bred in-house. Myeloid/Macrophage reporter animals were generated by crossing the LysM-Cre positive animal (see Jax Stock#: 004781) with the tdTomato (tdTom) reporter mouse (B6.Cg-Gt(ROSA)26Sor$^{tm14(CAG\text{-}tdTomato)Hze}$/J) purchased from The Jackson Laboratory (Stock#: 007914). Myeloid/Macrophage specific p75NTR knockout animals were generated by crossing the tamoxifen inducible LysM-CreERT2 animal (Jax 031674) to the p75NTRfl/fl animal that was kindly donated to us by Dr. Sung Yoon at the Ohio State University. All procedures were approved by the CCHMC Institutional Animal Care and Use Committee in compliance with AALAC approved practices.

Behavioral Measures. Neonatal animals were transferred from their home cage to opaque chambers fitted with a translucent lid. They were acclimated for 10 minutes prior to any assessments. Adolescent animals were transferred from their home cage to raised chambers fitted with black side walls, translucent viewing front, back and lids, and a grid mesh bottom. These animals were acclimated for 30 minutes prior to any assessments. Behavioral data were gathered at neonatal baseline and one day (1d) following early life injury. Further data was gathered at adolescent baseline and 1d, 3d, 7d, 14d and 21d following adolescent injury. Behavioral assessments were performed as described before[5] and below, and included a measure of spontaneous pain-like behavior as well as evoked muscle squeezing pain-like behavior.

Spontaneous pain-like behavior was measured as described previously by qualitatively assessing paw weight preference on a scale of zero to two, where zero is no guarding after injury, 1 indicates a shift in weight off of the injured paw, and 2 indicates a complete removal of the injured paw from the platform[5]. Assessments were made for a duration of 1 minute every 5 minutes for 30 minutes (neonates) or 1 hour (adolescents).

Muscle-directed withdrawal scores were measured using a digital pressure device (IITC Life Science Inc. Woodland Hills, CA, USA) with a dulled probe attachment ~2 mm wide at the tip. In this assay, the animal was lightly scruffed and was held upright. One at a time, the hind paws were inserted between the two arms of the device. The top arm has a flat platform to hold the dorsal hindpaw in place, while the bottom has the dulled probe. Slowly, the medial plantar paw was pressed by the probe while the animal and force were observed. When the animal gave a robust withdrawal response, the force in grams was recorded. This was repeated for a total of

three trials for each animal, separated by at least 5 minutes between trials for recovery. The maximum squeezing force implemented to a neonate was 150 grams and for an adolescent was 350 grams.

Injections. To induce cell apoptosis in MaFIA animals, the designed drug AP20187 (AP; B/B Homodimerizer purchased from Takara #635058) was first prepared according to manufacturer's directions in 100% ethanol. Prior to each experiment, fresh vehicle was prepared according to manufacturer's directions for 10 mg/kg which contained 10% PEG-400, 86% Tween and 4% drug/vehicle. All animals were injected with a final volume of 30 µL by intraperitoneal (IP) injections. The drug or vehicle was added to the mixture immediately before injecting the animal. AP20187 has no known impact on wildtype (WT) animals and previous reports demonstrate that neonates injected at P1, P2, P3 and P7 show robust knockout of Csf1r expressing cells in tissue[39,97]. Tamoxifen (1000 µg at 10 mg/mL) was injected in all animals within a litter of potential LysM-CreERT2;p75NTRfl/fl genotype. The injection protocol began at P33 and was completed i.p. daily for 5 days. Animals injected with Evan's Blue Dye (EBD, Sigma E2129-10) were injected as adolescence 16-20 hours prior to dissection with 200 µL of 1% EBD in sterile 0.9% saline.

Surgical Hind Paw Incisions. Animals were anesthetized with 2-3% isoflurane. Once sufficiently anesthetized, animals were placed on their backs and their right hind paw was taped to a sterile cloth. The dorsal skin was disinfected using Chlorhaxiderm Scrub and 70% isopropyl alcohol. A longitudinal incision was made through the hairy skin lateral to the main saphenous innervation territory. The incision was continued in between the bones through to the body of the flexor digitorum brevis muscles. The muscles were then manipulated using blunt dissection

techniques with #5 (neonate) and #3 (adolescent) forceps. The plantar skin was left untouched. The skin was sutured using 7-0 or 6-0 sutures for neonates and adolescents, respectively. Sham surgeries were performed exactly the same, except animals received only a suture through intact hairy hindpaw skin with no incision. Dual incision regimes were performed at both P7 and P35-P42 to the same hindpaw muscle.

Dissections. For peripheral sites, the animal was heavily anesthetized with ketamine and xylazine (100 and 16 mg/kg, respectively) and the tissue was removed. This included hind paw muscle, tibia, potineal lymph node and spleen. For neural tissue, the animal was first cardiac perfused with ice-cold saline prior to dissection where ipsilateral DRGs were removed.

Realtime PCR and Protein Arrays. RNA was isolated from BMDM cultures at the indicated time points using RNeasy Mini Kits (Qiagen Stock#: 74104). All isolation were performed exactly according to the manufacturer's instructions. 500ng of RNA was reverse transcribed to cDNA and realtime PCR was performed using SYBR Green Master Mix on a StepOne realtime PCR system (Applied Biosystems). Quantitative PCR was analyzed by the ΔΔcycle threshold (CT) method with normalization to GAPDH. Differences in expression and standard error are determined from the normalized ΔΔCt. This is used to calculate fold change between conditions and values are then converted to a percent change where 2-fold = 100% change[98]. Cytokines from BMDMs were analyzed using proteome profilers (R&D Systems ARY006) loaded with 700 µLs of media. One membrane was removed due to a lack of positive control expression (siCON stim LPS+IFNy). Data was first normalized to the average positive control before percent change from experimental control was calculated.

ATAC-Seq and RNA-seq. Peritoneal macrophages were isolated as indicated below from P7 naïve, P35 naïve, and P7 incised isolated at P35 animals. Samples were pooled across two animals of the same age and sex. Samples for ATAC- and RNA-Seq were processed by the sequencing core at CCHMC. Data were analyzed by the Bioinformatics Collaborative Services at CCHMC. Briefly, shared peaks between samples were obtained by merging peaks at 50% overlap with BEDtools v2.27.0 between replicates (peaks in all biological replicates) and treatment (merge at 50% all replicate peaks). These were then converted to Gene Transfer Format and peaks were counted with feature counts v1.6.2 (Rsubread package). Raw counts were normalized as transcripts per million and peaks were annotated by the nearest or overlapping gene and genomic features using an in-house script defined by: Promoter = 1kb upstream and downstream from peak; upstream = between 21 and 1kb from peak; priority = promoter>upstream>exon>intron. The R package DESeq2 v1.26.0 was used for differential analysis, with significance set to log2 fold change of 0.58 and FDR less than or equal to 0.05. RNA-seq was prepared similarly, where FASTQ formats were aligned to mm9 by STAR v2.6.le and stripped of duplicates by Sambamba v0.6.8. Read counts and differential expression were defined as before. Plots were generated by ggplot2 or PlotsReasy from CCHMC.

Immunohistochemistry. Freshly dissected tissue was frozen in OCT medium on dry ice or snap frozen in liquid N_2 for skeletal muscle and was then stored at -80ºC. On a cryostat, tissue was sectioned at 20 µm and was melted onto a slide. Tissue was fixed in 4% paraformaldehyde, washed and blocked prior to primary antibody (WGA 1:500 (Invitrogen W32466); Dystrophin 1:250 (Abcam ab15277); p75NTR 1:1000 (Cell Signaling 82385); F4/80 1:500 (Abcam ab6640)) incubation overnight. The next day, the tissue was washed and stained with secondary antibodies before cover slipping and stained with DAPI (Fisher Scientific 17985-50.) For tissue

that was genetically marked with a fluorescent dye, the tissue was post-fixed, washed, and mounted with media containing DAPI. Analysis was completed on Nikon's NIS Elements where two nonconsecutive sections across two slides was averaged to create a score for each animal.

Macrophage Isolation. *Peritoneal:* Animals were rapidly killed by cervical dislocation and cleaned with 70% ethanol. The peritoneum was injected with 1 mL (neonate) or 5 mLs (adolescent) of 3% fetal bovine serum (FBS) until bloated. The midsection was gently massaged to dislodge any cells, and then peritoneal fluid was extracted. Extracted peritoneal serum was processed for RNA extraction immediately, or sorted by the Flow Cytometry core at CCHMC by the LysMtdTom or MaFIA (GFP+) expression depending on the experiment and animal used. Cells were sorted in 2% FBS and into 50% FBS or PBS. Dead cells were marked with 7AAD and were removed from selection. Gating strategies were placed by the flow core and examples are presented.

Bone marrow derived macrophages (BMDM): Animals were prepared as above. The right leg was then detached from the body and placed into a dish containing HBSS. The femur and tibia were isolated, and the bone marrow was visualized by making horizontal cuts on either side of the knee. The bone marrow was flushed out of the bone with HBSS and a 22-gauge needle. HBSS with cells was collected, spun at 4ºC and 1500 RPM for 5 minutes. The supernatant was discarded, and RPMI buffer (Catalog #11875093) supplemented with 10% fetal bovine serum (35-010-CV Lot 35010171) and gentamycin was added to resuspend the cells. GM-CSF (2 µg/mL) was added, and cells were incubated for 5 days at 37ºC and 5% CO_2. Additional media and GM-CSF was added halfway through the incubation. After maturation, cells were treated with siRNAs (Origene 10 ng/uL) and stimulants (NGF, BDNF 50 ng/uL or LPS+IFNγ 10 ng/uL

each) as indicated in the figure legends. Knockdown efficiency tested across three duplexes, achieved 90% by PCR. Cells were stimulated for 24 hours before washing, trypsinizing, and/or scraping of the plates. Media was saved for protein array analyses. Cells were counted using a hemocytometer and then resuspended in buffer for RNA isolation using the RNeasy Mini Kit.

Adoptive Transfer. Peritoneal macrophages from MaFIA animals were isolated as described above. ~80k cells were sorted into PBS. These were pelleted and reconstituted in 10 µLs of sterile PBS. Naïve hosts were anesthetized and the right hindpaw was injected with all of the cells directly into either intact muscle, or the wound of a hindpaw incision before suturing. Animals were monitored following the transplant for adverse effects and behavioral responses.

Bone Marrow Transplant. Tibia and femur bone marrow was collected using sterile tools from adolescent animals. Under a sterile hood, bones were flushed with PBS and treated with red blood cell lysis buffer until a transparent pellet was formed after centrifugation at 1100 RMP for 4 minutes at 4ºC. After reconstitution, cells were passed through a 70 µm filter and were counted on a hemocytometer. One million cells were transferred to a naïve age and sex matched host that was previously exposed to radiation (administered in split doses, the first at 700 rads/700 cGy followed 3 hours later with a second dose of 4.75 Gy (475 rads/475 cGy)) to prepare for the transplant. Animals were monitored following the transplant in their immune compromised state. We successfully completed 28 out of 32 BMTs. The animals were allowed to recover for 16 weeks prior to further experimentation, to ensure a functional immune response after transplant[99,100].

Human induced pluripotent stem cell preparations and calcium imaging. Human induced pluripotent stem cells (iPSC) derived CD14+ monocytes (ATCC, Manassas, VA, Cat No. DYS0100) were plated in macrophage differentiation medium (RPMI-1640 Medium /10% Fetal Bovine Serum (FBS), supplemented with 100 ng/ml human M-CSF, and 1% Pen/Strep) in 24 well plate at a density of 10^5 cells/ml according to manufacturer's directions. Monocytes were differentiated into macrophages within seven days. Half medium change and siRNA treatment were done at day three and day five, respectively. Briefly, 10 nM control (siCON), or siRNAs against p75NTR (sip75; Origene SR321107) were incubated with macrophages at day five in macrophage differentiation medium. At day six, macrophages treated with siRNAs were stimulated with either 50 ng/ml NGF or vehicle in macrophage differentiation medium for 24 hours. At day seven, the media was extracted and used for stimulation of the sensory neurons.

Human iPSC-Derived Sensory Neuron Progenitors (AXOL; ax0555) were cultured on SureBond-XF-coated 96 well plate with Neural Plating Medium (AXOL, product codes: ax0053 and ax0033) for 24 hours as recommended by the manufacturer. Briefly, full media change was achieved by replacing the neural plating medium with sensory neuron maintenance medium supplemented with growth factors (25 ng/mL Glial-Derived Neurotrophic Factor (ax139855), 25 ng/mL Nerve Growth Factor (ax139789), 10 ng/mL Brain-Derived Neurotrophic Factor (ax139800), and 10 ng/mL Neurotrophin-3 (ax139811) and sensory maturation maximizer (ax0058) at a seeding density of 50000/cm^2. Cells were treated with 2.5 µg/ml mitomycin C at day three after which the media was replaced with sensory neuron maintenance medium supplemented with growth factors and sensory maturation maximizer. Half media change was done at every three days for 21 days. All iPSC cultures and incubations were carried out in 5% CO_2/ 37°C.

For imaging, cells were pretreated with 5 µg/ml Rhodamine (in DMSO, ThermoFisher R1244) for 30-45 minutes and further dosed with equal volume of siRNA treated and stimulated macrophage media. Neuronal activities were visualized using wide-field Nikon Ti2 inverted SpectraX with 10X LWD Phase high quality objective. To analyze changes in fluorescence, regions of interest (ROI) were randomly drawn around 15 cells across triplicate conditions. Calcium transients were measured for after stimulation with ATP (200µM) followed by capsaicin (1µM). ΔF/FO were calculated where ΔF/FO = (Fmax – FO) / FO where Fmax: maximum intensity during stimulation and FO: the average intensity of immediately prior to stimulation.

***Ex vivo* Preparation.** This preparation has recently been described in detail[88]. In this study, pups were treated with either AP or vehicle as described above and were subjected to a P7 incision followed by a P35-P42 incision. Briefly, 7d after the second incision we dissected the animal HP muscle/tibial nerve/DRG/SC in continuity in ice cold oxygenated (95%O2/5% CO2) artificial cerebral spinal fluid (aCSF; 127.0 mM NaCl, 1.9mM KC l, 1.2 mM KH2PO4, 1.3 mM MgSO4, 2.4 mM CaCl2, 26.0 mM NaHCO3, and 10.0 mM D-glucose: O2aCSF). The preparation was transferred to a new dish where the muscle and DRGs were isolated in separate circulating baths of O2aCSF. The temperature was slowly raised to 32ºC. In L3 or L4 an electrode was filled with 5% neurobiotin and 1M potassium acetate for sharp electrode single unit recordings using Quartz electrodes (impedance>150MΩ). A suction electrode was placed on the side of the tibial nerve to send search stimuli. An impaled cell was identified by the presence of an action potential (AP) recording from the search stimulus. A receptive field on the muscle was then located using a concentric bipolar electrode. If found, the cell was counted in our analyses and mechanical, thermal and chemical stimuli were applied in that order. First von Frey fiber thresholds were identified using fibers from 0.07-10g of force applied for ~1-2 seconds. If the cell did not respond to the maximum, physical push was applied to determine if

the cell would respond to any mechanical force. Next ice-cold saline (~2ºC) was applied to the circulating bath over the receptive field, followed by hot ~53ºC saline. After washout, a low concentration mixture of lactic acid, protons and ATP (applied just before stimulation) were oxygenated and flooded the muscle chamber through an in-line heater for 2 minutes (15 mM lactate, 1μM ATP, pH 7.0). This was repeated with a high concentration of the same metabolites (50 mM lactate, 5 μM ATP, pH 6.6). Mechanical and thermal responses were then repeated.

Activity was recorded by the Spike2 program (Cambridge Electronic Design) and was analyzed offline. At the end of the preparation the nerve length from suction electrode to DRG was measured to calculate conduction velocity (CV), where a Group IV afferent was defined as being (≤1.2 m/s) or Group III afferents (1.2–14 m/s). Mechanical thresholds were set at the minimum force required to evoke an action potential, firing rate (FR) was calculated as the maximum number events that occurred over a 200 ms bin, and instantaneous frequency (IF) was calculated to determine the maximum response to a stimulus. Distribution analyses were completed to determine if there was a shift in the number of responders in our conditions.

Statistical Analyses. Data was analyzed using SigmaPlot software (v14.5). Critical significance value was set to $\alpha<0.05$. All data were first checked for normality by Shapiro-Wilk to determine parametric or nonparametric tests. Individual tests used are described in the figure legends. Behavioral data of the same animal over time and between groups were analyzed using a two-way repeated measures (RM) ANOVA. In situations in which different animals were compared across multiple time points and groups, such as PCR data, a two-way ANOVA was used. Data at a single time points across multiple groups including much of the electrophysiological data were analyzed by a one-way ANOVA. Proportions data were analyzed

using a Chi-squared or Fisher's exact test as marked in the figure legends. Graphs were made using GraphPad Prism (v9). In all experiments in which there is a potential for bias including behavior, electrophysiology, cell culture and IHC the investigator was blinded to the conditions. For behavior, animals were assigned to groups by a random number generator. Biological and technical replicates were completed for each experiment and are appropriately marked in the figure legends.

References.

1 Udit, S., Blake, K. & Chiu, I. M. Somatosensory and autonomic neuronal regulation of the immune response. *Nature Reviews Neuroscience* **23**, 157-171 (2022). https://doi.org:10.1038/s41583-021-00555-4

2 Tamari, M., Ver Heul, A. M. & Kim, B. S. Immunosensation: Neuroimmune Cross Talk in the Skin. *Annu Rev Immunol* (2021). https://doi.org:10.1146/annurev-immunol-101719-113805

3 Karshikoff, B., Tadros, M. A., Mackey, S. & Zouikr, I. Neuroimmune modulation of pain across the developmental spectrum. *Current opinion in behavioral sciences* **28**, 85-92 (2019). https://doi.org:10.1016/j.cobeha.2019.01.010

4 Spencer, S. J., Galic, M. A. & Pittman, Q. J. Neonatal programming of innate immune function. *Am J Physiol Endocrinol Metab* **300**, E11-18 (2011). https://doi.org:10.1152/ajpendo.00516.2010

5 Dourson, A. J. *et al.* Early Life Nociception is Influenced by Peripheral Growth Hormone Signaling. *The Journal of neuroscience : the official journal of the Society for Neuroscience* (2021). https://doi.org:10.1523/jneurosci.3081-20.2021

6 Fitzgerald, M. The development of nociceptive circuits. *Nature Reviews Neuroscience* **6**, 507-520 (2005). https://doi.org:10.1038/nrn1701

7 Jankowski, M. P. *et al.* Age-dependent sensitization of cutaneous nociceptors during developmental inflammation. *Molecular pain* **10**, 34 (2014). https://doi.org:10.1186/1744-8069-10-34

8 Jones, L. *et al.* Widespread nociceptive maps in the human neonatal somatosensory cortex. *eLife* **11**, e71655 (2022). https://doi.org:10.7554/eLife.71655

9 Kumar, S. K. & Bhat, B. V. Distinct mechanisms of the newborn innate immunity. *Immunology letters* **173**, 42-54 (2016). https://doi.org:10.1016/j.imlet.2016.03.009

10 Winterberg, T. *et al.* Distinct phenotypic features of neonatal murine macrophages. *European journal of immunology* **45**, 214-224 (2015). https://doi.org:10.1002/eji.201444468

11 Walker, S. M. *et al.* Somatosensory function and pain in extremely preterm young adults from the UK EPICure cohort: sex-dependent differences and impact of neonatal surgery. *British journal of anaesthesia* **121**, 623-635 (2018). https://doi.org:10.1016/j.bja.2018.03.035

12 Hermann, C., Hohmeister, J., Demirakca, S., Zohsel, K. & Flor, H. Long-term alteration of pain sensitivity in school-aged children with early pain experiences. *Pain* **125**, 278-285 (2006). https://doi.org:10.1016/j.pain.2006.08.026

13 Moriarty, O., Harrington, L., Beggs, S. & Walker, S. M. Opioid analgesia and the somatosensory memory of neonatal surgical injury in the adult rat. *British journal of anaesthesia* **121**, 314-324 (2018). https://doi.org:10.1016/j.bja.2017.11.111

14 Fragiadakis, G. K. *et al.* Patient-specific Immune States before Surgery Are Strong Correlates of Surgical Recovery. *Anesthesiology* **123**, 1241-1255 (2015). https://doi.org:10.1097/aln.0000000000000887

15 Laudanski, K. *et al.* Acquired immunological imbalance after surgery with cardiopulmonary bypass due to epigenetic over-activation of PU.1/M-CSF. *J Transl Med* **16**, 143 (2018). <https://www.ncbi.nlm.nih.gov/pmc/articles/PMC5970449/pdf/12967_2018_Article_1518.pdf> .

16 Koennecke, L. A., Zito, M. A., Proescholdt, M. G., van Rooijen, N. & Heyes, M. P. Depletion of systemic macrophages by liposome-encapsulated clodronate attenuates increases in brain quinolinic acid during CNS-localized and systemic immune activation. *Journal of neurochemistry* **73**, 770-779 (1999).

17 Shutov, L. P. *et al.* The Complement System Component C5a Produces Thermal Hyperalgesia via Macrophage-to-Nociceptor Signaling That Requires NGF and TRPV1. *The Journal of neuroscience : the official journal of the Society for Neuroscience* **36**, 5055-5070 (2016). https://doi.org:10.1523/jneurosci.3249-15.2016

18 Wang, Y. R., Mao, X. F., Wu, H. Y. & Wang, Y. X. Liposome-encapsulated clodronate specifically depletes spinal microglia and reduces initial neuropathic pain. *Biochemical and biophysical research communications* **499**, 499-505 (2018). https://doi.org:10.1016/j.bbrc.2018.03.177

19 Mert, T. *et al.* Macrophage depletion delays progression of neuropathic pain in diabetic animals. *Naunyn-Schmiedeberg's archives of pharmacology* **379**, 445-452 (2009). https://doi.org:10.1007/s00210-008-0387-3

20 Shepherd, A. J. *et al.* Angiotensin II Triggers Peripheral Macrophage-to-Sensory Neuron Redox Crosstalk to Elicit Pain. *The Journal of neuroscience : the official journal of the Society for Neuroscience* **38**, 7032-7057 (2018). https://doi.org:10.1523/jneurosci.3542-17.2018

21 Shepherd, A. J. *et al.* Macrophage angiotensin II type 2 receptor triggers neuropathic pain. *Proceedings of the National Academy of Sciences of the United States of America* **115**, E8057-E8066 (2018). https://doi.org:10.1073/pnas.1721815115

22 Pannell, M. *et al.* Adoptive transfer of M2 macrophages reduces neuropathic pain via opioid peptides. *Journal of neuroinflammation* **13**, 262 (2016). https://doi.org:10.1186/s12974-016-0735-z

23 Jupelli, M. *et al.* Chlamydia pneumoniae infection in mice induces chronic lung inflammation, iBALT formation, and fibrosis. *PloS one* **8**, e77447 (2013). https://doi.org:10.1371/journal.pone.0077447

24 Bermick, J. R. *et al.* Neonatal monocytes exhibit a unique histone modification landscape. *Clinical epigenetics* **8**, 99 (2016). https://doi.org:10.1186/s13148-016-0265-7

25 Norouzitallab, P., Baruah, K., Biswas, P., Vanrompay, D. & Bossier, P. Probing the phenomenon of trained immunity in invertebrates during a transgenerational study, using brine shrimp Artemia as a model system. *Sci Rep* **6**, 21166 (2016). https://doi.org:10.1038/srep21166

26 Netea, M. G. *et al.* Trained immunity: A program of innate immune memory in health and disease. *Science (New York, N.Y.)* **352**, aaf1098 (2016). https://doi.org:10.1126/science.aaf1098

27 Fitzgerald, M. Developmental biology of inflammatory pain. *British journal of anaesthesia* **75**, 177-185 (1995). https://doi.org:10.1093/bja/75.2.177

28 Bracci-Laudiero, L. & De Stefano, M. E. in *Neurotoxin Modeling of Brain Disorders—Life-long Outcomes in Behavioral Teratology* (eds Richard M. Kostrzewa & Trevor Archer) 125-152 (Springer International Publishing, 2016).

29 Kobayashi, H. & Mizisin, A. P. Nerve growth factor and neurotrophin-3 promote chemotaxis of mouse macrophages in vitro. *Neuroscience letters* **305**, 157-160 (2001). https://doi.org:10.1016/s0304-3940(01)01854-7
30 Sajanti, A. *et al.* A comprehensive p75 neurotrophin receptor gene network and pathway analyses identifying new target genes. *Scientific Reports* **10**, 14984 (2020). https://doi.org:10.1038/s41598-020-72061-z
31 Chen, Z. *et al.* p75 Is Required for the Establishment of Postnatal Sensory Neuron Diversity by Potentiating Ret Signaling. *Cell Rep* **21**, 707-720 (2017). https://doi.org:10.1016/j.celrep.2017.09.037
32 Dourson, A. J. *et al.* Genetic and epigenetic mechanisms influencing acute to chronic postsurgical pain transitions in pediatrics: Preclinical to clinical evidence. *Canadian Journal of Pain*, null-null (2022). https://doi.org:10.1080/24740527.2021.2021799
33 Fortier, M. A., MacLaren, J. E., Martin, S. R., Perret-Karimi, D. & Kain, Z. N. Pediatric pain after ambulatory surgery: where's the medication? *Pediatrics* **124**, e588-595 (2009). https://doi.org:10.1542/peds.2008-3529
34 Rabbitts, J. A., Fisher, E., Rosenbloom, B. N. & Palermo, T. M. Prevalence and Predictors of Chronic Postsurgical Pain in Children: A Systematic Review and Meta-Analysis. *J Pain* **18**, 605-614 (2017). https://doi.org:10.1016/j.jpain.2017.03.007
35 Neville, A. *et al.* Diagnostic uncertainty in pediatric chronic pain: nature, prevalence, and consequences. *Pain reports* **5**, e871 (2020). https://doi.org:10.1097/pr9.0000000000000871
36 Angst, M. S. *et al.* Aversive and reinforcing opioid effects: a pharmacogenomic twin study. *Anesthesiology* **117**, 22-37 (2012). https://doi.org:10.1097/ALN.0b013e31825a2a4e
37 Martin, L., Jimenez, N. & Lynn, A. A review of perioperative anesthesia and analgesia for infants: updates and trends to watch [version 1; referees: 2 approved]. *F1000Research* **6** (2017). https://doi.org:10.12688/f1000research.10272.1
38 Yu, X. *et al.* Dorsal root ganglion macrophages contribute to both the initiation and persistence of neuropathic pain. *Nat Commun* **11**, 264 (2020). https://doi.org:10.1038/s41467-019-13839-2
39 Kalymbetova, T. V. *et al.* Resident alveolar macrophages are master regulators of arrested alveolarization in experimental bronchopulmonary dysplasia. *The Journal of pathology* **245**, 153-159 (2018). https://doi.org:10.1002/path.5076
40 Burnett, S. H. *et al.* Conditional macrophage ablation in transgenic mice expressing a Fas-based suicide gene. *Journal of leukocyte biology* **75**, 612-623 (2004). https://doi.org:10.1189/jlb.0903442
41 Geissmann, F. *et al.* Development of monocytes, macrophages, and dendritic cells. *Science (New York, N.Y.)* **327**, 656-661 (2010). https://doi.org:10.1126/science.1178331
42 Lissner, M. M. *et al.* Age-Related Gene Expression Differences in Monocytes from Human Neonates, Young Adults, and Older Adults. *PloS one* **10**, e0132061 (2015). https://doi.org:10.1371/journal.pone.0132061
43 Millay, D. P. *et al.* Genetic and pharmacologic inhibition of mitochondrial-dependent necrosis attenuates muscular dystrophy. *Nature medicine* **14**, 442-447 (2008). https://doi.org:10.1038/nm1736
44 Jankowski, M. P., Rau, K. K., Ekmann, K. M., Anderson, C. E. & Koerber, H. R. Comprehensive phenotyping of group III and IV muscle afferents in mouse. *Journal of neurophysiology* **109**, 2374-2381 (2013). https://doi.org:10.1152/jn.01067.2012
45 Koerber, H. R. *et al.* Cutaneous C-polymodal fibers lacking TRPV1 are sensitized to heat following inflammation, but fail to drive heat hyperalgesia in the absence of TPV1 containing C-heat fibers. *Molecular pain* **6**, 58 (2010). https://doi.org:10.1186/1744-8069-6-58

46 Follis, R. M. *et al.* Metabolic Control of Sensory Neuron Survival by the p75 Neurotrophin Receptor in Schwann Cells. *The Journal of neuroscience : the official journal of the Society for Neuroscience* **41**, 8710-8724 (2021). https://doi.org:10.1523/jneurosci.3243-20.2021

47 Subramanian Vignesh, K., Landero Figueroa, J. A., Porollo, A., Caruso, J. A. & Deepe, G. S., Jr. Granulocyte macrophage-colony stimulating factor induced Zn sequestration enhances macrophage superoxide and limits intracellular pathogen survival. *Immunity* **39**, 697-710 (2013). https://doi.org:10.1016/j.immuni.2013.09.006

48 dos Santos, N. L. *et al.* Age and Sex Drive Differential Behavioral and Neuroimmune Phenotypes During Postoperative Pain. *Neurobiology of Aging* (2022). https://doi.org:https://doi.org/10.1016/j.neurobiolaging.2022.09.008

49 Spencer, S. J., Martin, S., Mouihate, A. & Pittman, Q. J. Early-life immune challenge: defining a critical window for effects on adult responses to immune challenge. *Neuropsychopharmacology : official publication of the American College of Neuropsychopharmacology* **31**, 1910-1918 (2006). https://doi.org:10.1038/sj.npp.1301004

50 Reynolds, M. L. & Fitzgerald, M. Long-term sensory hyperinnervation following neonatal skin wounds. *The Journal of comparative neurology* **358**, 487-498 (1995). https://doi.org:10.1002/cne.903580403

51 Walker, S. M., Meredith-Middleton, J., Cooke-Yarborough, C. & Fitzgerald, M. Neonatal inflammation and primary afferent terminal plasticity in the rat dorsal horn. *Pain* **105**, 185-195 (2003).

52 Walker, S. M. Long-term effects of neonatal pain. *Seminars in fetal & neonatal medicine* (2019). https://doi.org:10.1016/j.siny.2019.04.005

53 Walker, S. M. Early life pain—effects in the adult. *Current Opinion in Physiology* **11**, 16-24 (2019). https://doi.org:https://doi.org/10.1016/j.cophys.2019.04.011

54 Zhong, X. S. *et al.* Neonatal Colonic Inflammation Epigenetically Aggravates Epithelial Inflammatory Responses to Injury in Adult Life. *Cellular and molecular gastroenterology and hepatology* **6**, 65-78 (2018). https://doi.org:10.1016/j.jcmgh.2018.02.014

55 Chidambaran, V. *et al.* Enrichment of Genomic Pathways Based on Differential DNA Methylation Associated With Chronic Postsurgical Pain and Anxiety in Children: A Prospective, Pilot Study. *J Pain* **20**, 771-785 (2019). https://doi.org:10.1016/j.jpain.2018.12.008

56 Brewer, C. L., Li, J., O'Conor, K., Serafin, E. K. & Baccei, M. L. Neonatal Injury Evokes Persistent Deficits in Dynorphin Inhibitory Circuits within the Adult Mouse Superficial Dorsal Horn. *The Journal of neuroscience : the official journal of the Society for Neuroscience* **40**, 3882-3895 (2020). https://doi.org:10.1523/jneurosci.0029-20.2020

57 Moriarty, O. *et al.* Priming of Adult Incision Response by Early-Life Injury: Neonatal Microglial Inhibition Has Persistent But Sexually Dimorphic Effects in Adult Rats. *The Journal of Neuroscience* **39**, 3081 (2019). https://doi.org:10.1523/JNEUROSCI.1786-18.2019

58 van den Hoogen, N. J. *et al.* Repeated touch and needle-prick stimulation in the neonatal period increases the baseline mechanical sensitivity and postinjury hypersensitivity of adult spinal sensory neurons. *Pain* **159**, 1166-1175 (2018). https://doi.org:10.1097/j.pain.0000000000001201

59 Schwaller, F., Beggs, S. & Walker, S. M. Targeting p38 Mitogen-activated Protein Kinase to Reduce the Impact of Neonatal Microglial Priming on Incision-induced Hyperalgesia in the Adult Rat. *Anesthesiology* **122**, 1377-1390 (2015). https://doi.org:10.1097/aln.0000000000000659

60 Beggs, S., Currie, G., Salter, M. W., Fitzgerald, M. & Walker, S. M. Priming of adult pain responses by neonatal pain experience: maintenance by central neuroimmune activity. *Brain* **135**, 404-417 (2012). https://doi.org:10.1093/brain/awr288

61 Kato, J. & Svensson, C. I. in *Progress in Molecular Biology and Translational Science* Vol. 131 (eds Theodore J. Price & Gregory Dussor) 251-279 (Academic Press, 2015).
62 Comish, P. B., Carlson, D., Kang, R. & Tang, D. Damage-Associated Molecular Patterns and the Systemic Immune Consequences of Severe Thermal Injury. *The Journal of Immunology* **205**, 1189 (2020). https://doi.org:10.4049/jimmunol.2000439
63 McMahon, S. B., Cafferty, W. B. & Marchand, F. Immune and glial cell factors as pain mediators and modulators. *Experimental neurology* **192**, 444-462 (2005). https://doi.org:10.1016/j.expneurol.2004.11.001
64 Basbaum, A. I., Bautista, D. M., Scherrer, G. & Julius, D. Cellular and molecular mechanisms of pain. *Cell* **139**, 267-284 (2009). https://doi.org:10.1016/j.cell.2009.09.028
65 Ren, K. & Dubner, R. Interactions between the immune and nervous systems in pain. *Nature medicine* **16**, 1267-1276 (2010). https://doi.org:10.1038/nm.2234
66 Philippou, A., Maridaki, M., Theos, A. & Koutsilieris, M. Cytokines in muscle damage. *Advances in clinical chemistry* **58**, 49-87 (2012). https://doi.org:10.1016/b978-0-12-394383-5.00010-2
67 Campero, M., Bostock, H., Baumann, T. K. & Ochoa, J. L. Activity-dependent slowing properties of an unmyelinated low threshold mechanoreceptor in human hairy skin. *Neuroscience letters* **493**, 92-96 (2011). https://doi.org:10.1016/j.neulet.2011.02.012
68 McKelvey, R., Berta, T., Old, E., Ji, R.-R. & Fitzgerald, M. Neuropathic Pain Is Constitutively Suppressed in Early Life by Anti-Inflammatory Neuroimmune Regulation. *The Journal of Neuroscience* **35**, 457-466 (2015). https://doi.org:10.1523/jneurosci.2315-14.2015
69 Wallner, S. *et al.* Epigenetic dynamics of monocyte-to-macrophage differentiation. *Epigenetics & chromatin* **9**, 33 (2016). https://doi.org:10.1186/s13072-016-0079-z
70 Foster, S. L., Hargreaves, D. C. & Medzhitov, R. Gene-specific control of inflammation by TLR-induced chromatin modifications. *Nature* **447**, 972-978 (2007). https://doi.org:10.1038/nature05836
71 Lavin, Y. *et al.* Tissue-resident macrophage enhancer landscapes are shaped by the local microenvironment. *Cell* **159**, 1312-1326 (2014). https://doi.org:10.1016/j.cell.2014.11.018
72 Cobo, M. M. *et al.* Early life inflammation is associated with spinal cord excitability and nociceptive sensitivity in human infants. *Nature communications* **13**, 3943 (2022). https://doi.org:10.1038/s41467-022-31505-y
73 Pinho-Ribeiro, F. A. *et al.* Blocking Neuronal Signaling to Immune Cells Treats Streptococcal Invasive Infection. *Cell* **173**, 1083-1097.e1022 (2018). https://doi.org:10.1016/j.cell.2018.04.006
74 Perner, C. *et al.* Substance P Release by Sensory Neurons Triggers Dendritic Cell Migration and Initiates the Type-2 Immune Response to Allergens. *Immunity* **53**, 1063-1077.e1067 (2020). https://doi.org:https://doi.org/10.1016/j.immuni.2020.10.001
75 Filtjens, J. *et al.* Nociceptive sensory neurons promote CD8 T cell responses to HSV-1 infection. *Nat Commun* **12**, 2936 (2021). https://doi.org:10.1038/s41467-021-22841-6
76 Mendell, L. M. Neurotrophins and sensory neurons: role in development, maintenance and injury. A thematic summary. *Philosophical transactions of the Royal Society of London. Series B, Biological sciences* **351**, 463-467 (1996). https://doi.org:10.1098/rstb.1996.0043
77 Lewin, G. R., Ritter, A. M. & Mendell, L. M. On the role of nerve growth factor in the development of myelinated nociceptors. *The Journal of neuroscience : the official journal of the Society for Neuroscience* **12**, 1896-1905 (1992).
78 Sharma, N. *et al.* The emergence of transcriptional identity in somatosensory neurons. *Nature* **577**, 392-398 (2020). https://doi.org:10.1038/s41586-019-1900-1
79 Luo, W. *et al.* A hierarchical NGF signaling cascade controls Ret-dependent and Ret-independent events during development of nonpeptidergic DRG neurons. *Neuron* **54**, 739-754 (2007). https://doi.org:10.1016/j.neuron.2007.04.027

80 Susaki, Y. *et al.* Functional properties of murine macrophages promoted by nerve growth factor. *Blood* **88**, 4630-4637 (1996).
81 Williams, K. S., Killebrew, D. A., Clary, G. P., Seawell, J. A. & Meeker, R. B. Differential regulation of macrophage phenotype by mature and pro-nerve growth factor. *Journal of neuroimmunology* **285**, 76-93 (2015). https://doi.org:10.1016/j.jneuroim.2015.05.016
82 Khodorova, A., Nicol, G. D. & Strichartz, G. The p75NTR signaling cascade mediates mechanical hyperalgesia induced by nerve growth factor injected into the rat hind paw. *Neuroscience* **254**, 312-323 (2013). https://doi.org:10.1016/j.neuroscience.2013.09.046
83 Leitão, L. *et al.* Bone marrow cell response after injury and during early stage of regeneration is independent of the tissue-of-injury in 2 injury models. *The FASEB Journal* **33**, 857-872 (2019). https://doi.org:https://doi.org/10.1096/fj.201800610RR
84 Glatman Zaretsky, A., Engiles, J. B. & Hunter, C. A. Infection-induced changes in hematopoiesis. *Journal of immunology (Baltimore, Md. : 1950)* **192**, 27-33 (2014). https://doi.org:10.4049/jimmunol.1302061
85 Leitão, L. *et al.* The alliance between nerve fibers and stem cell populations in bone marrow: life partners in sickness and health. *The FASEB Journal* **33**, 8697-8710 (2019). https://doi.org:https://doi.org/10.1096/fj.201900454R
86 Cai, R. *et al.* Panoptic imaging of transparent mice reveals whole-body neuronal projections and skull–meninges connections. *Nature Neuroscience* **22**, 317-327 (2019). https://doi.org:10.1038/s41593-018-0301-3
87 Mazzitelli, J. A. *et al.* Cerebrospinal fluid regulates skull bone marrow niches via direct access through dural channels. *Nature Neuroscience* **25**, 555-560 (2022). https://doi.org:10.1038/s41593-022-01029-1
88 Queme, L. F. *et al.* Disruption of Hyaluronic Acid in Skeletal Muscle Induces Decreased Voluntary Activity via Chemosensitive Muscle Afferent Sensitization in Male Mice. *eNeuro* **9** (2022). https://doi.org:10.1523/eneuro.0522-21.2022
89 Walker, S. M., Tochiki, K. K. & Fitzgerald, M. Hindpaw incision in early life increases the hyperalgesic response to repeat surgical injury: critical period and dependence on initial afferent activity. *Pain* **147**, 99-106 (2009). https://doi.org:10.1016/j.pain.2009.08.017
90 Sorge, R. E. *et al.* Different immune cells mediate mechanical pain hypersensitivity in male and female mice. *Nat Neurosci* **18**, 1081-1083 (2015). https://doi.org:10.1038/nn.4053
91 Mogil, J. S. Qualitative sex differences in pain processing: emerging evidence of a biased literature. *Nature Reviews Neuroscience* **21**, 353-365 (2020). https://doi.org:10.1038/s41583-020-0310-6
92 Peters, J. W. *et al.* Does neonatal surgery lead to increased pain sensitivity in later childhood? *Pain* **114**, 444-454 (2005). https://doi.org:10.1016/j.pain.2005.01.014
93 Williams, M. D. & Lascelles, B. D. X. Early Neonatal Pain-A Review of Clinical and Experimental Implications on Painful Conditions Later in Life. *Front Pediatr* **8**, 30 (2020). https://doi.org:10.3389/fped.2020.00030
94 Malik, S. C. *et al.* In vivo functions of p75(NTR): challenges and opportunities for an emerging therapeutic target. *Trends Pharmacol Sci* **42**, 772-788 (2021). https://doi.org:10.1016/j.tips.2021.06.006
95 Norman, B. H. & McDermott, J. S. Targeting the Nerve Growth Factor (NGF) Pathway in Drug Discovery. Potential Applications to New Therapies for Chronic Pain. *J Med Chem* **60**, 66-88 (2017). https://doi.org:10.1021/acs.jmedchem.6b00964
96 Zhao, Z., Ukidve, A., Kim, J. & Mitragotri, S. Targeting Strategies for Tissue-Specific Drug Delivery. *Cell* **181**, 151-167 (2020). https://doi.org:https://doi.org/10.1016/j.cell.2020.02.001

97 Burnett, S. H. *et al.* Development of peritoneal adhesions in macrophage depleted mice. *The Journal of surgical research* **131**, 296-301 (2006). https://doi.org:10.1016/j.jss.2005.08.026

98 Queme, L. F., Weyler, A. A., Cohen, E. R., Hudgins, R. C. & Jankowski, M. P. A dual role for peripheral GDNF signaling in nociception and cardiovascular reflexes in the mouse. *Proc Natl Acad Sci U S A* **117**, 698-707 (2020). https://doi.org:10.1073/pnas.1910905116

99 May, M., Slaughter, A. & Lucas, D. Dynamic regulation of hematopoietic stem cells by bone marrow niches. *Curr Stem Cell Rep* **4**, 201-208 (2018). https://doi.org:10.1007/s40778-018-0132-x

100 Ojielo, C. I. *et al.* Defective phagocytosis and clearance of Pseudomonas aeruginosa in the lung following bone marrow transplantation. *Journal of immunology (Baltimore, Md. : 1950)* **171**, 4416-4424 (2003). https://doi.org:10.4049/jimmunol.171.8.4416

Figure 1

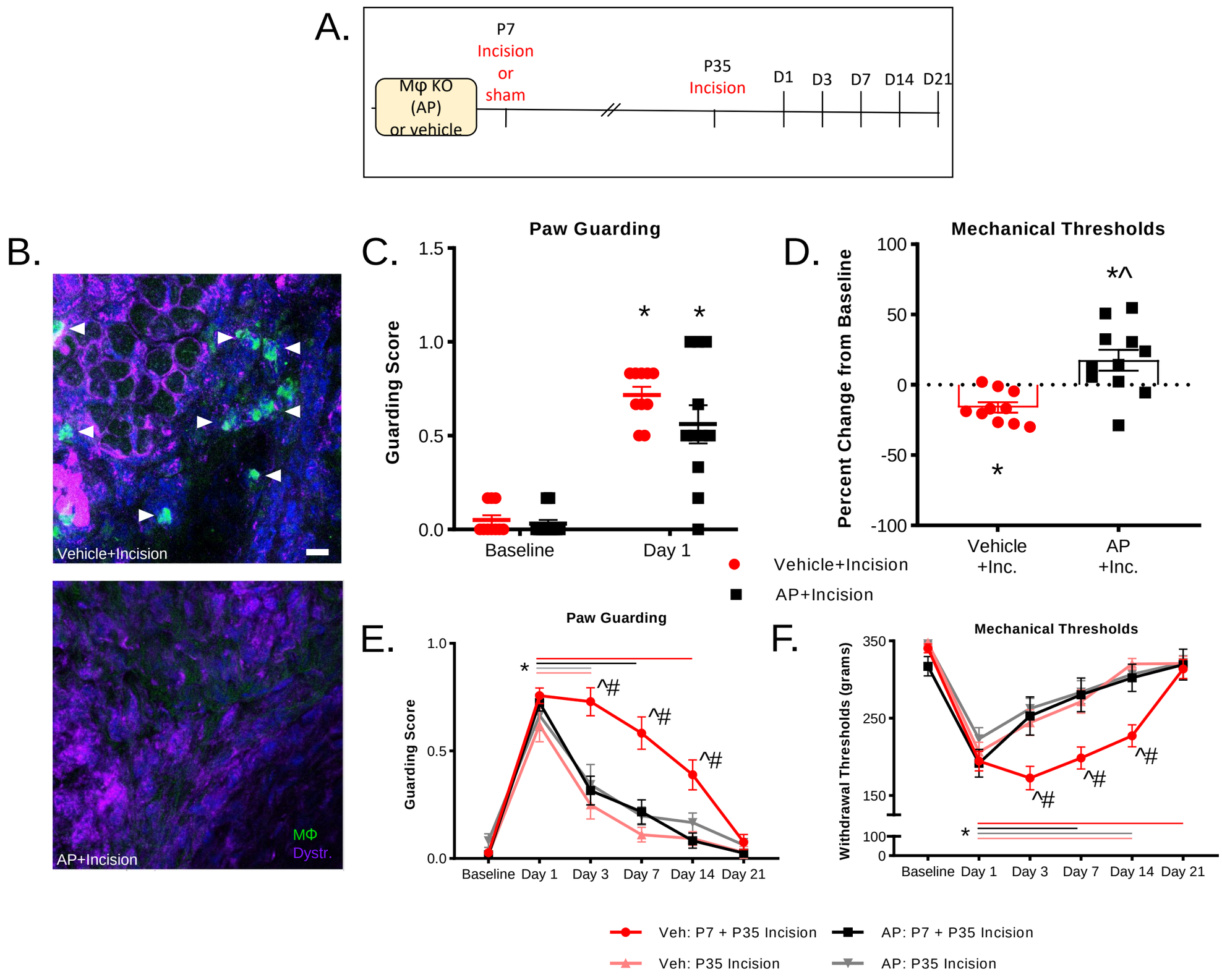
A.
P7
Incision
or
sham
Mφ KO
(AP)
or vehicle
P35
Incision
D1
D3
D7
D14
D21
B.
Vehicle+Incision
AP+Incision
MΦ
Dystr.
C.
Paw Guarding
Guarding Score
1.5
1.0
0.5
0.0
Baseline
Day 1
D.
Mechanical Thresholds
Percent Change from Baseline
100
50
0
-50
-100
Vehicle
+Inc.
AP
+Inc.
Vehicle+Incision
AP+Incision
E.
Paw Guarding
Guarding Score
Baseline
Day 1
Day 3
Day 7
Day 14
Day 21
F.
Mechanical Thresholds
Withdrawal Thresholds (grams)
350
250
150
100
0
Veh: P7 + P35 Incision
AP: P7 + P35 Incision
Veh: P35 Incision
AP: P35 Incision

Figure 2

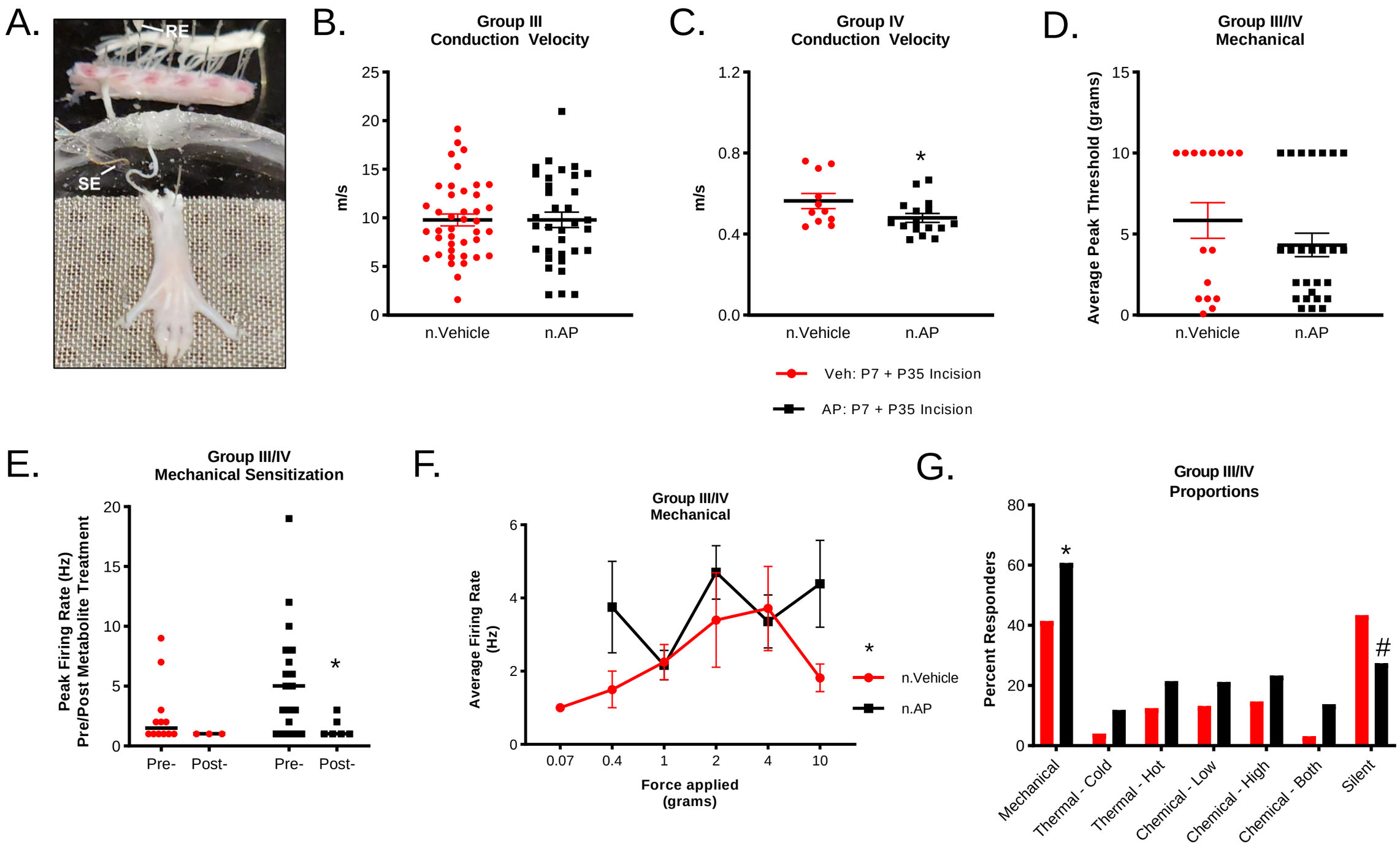
A.
RE
SE
B.
Group III
Conduction Velocity
m/s
25
20
15
10
5
0
n.Vehicle
n.AP
C.
Group IV
Conduction Velocity
m/s
1.2
0.8
0.4
0.0
*
n.Vehicle
n.AP
Veh: P7 + P35 Incision
AP: P7 + P35 Incision
D.
Group III/IV
Mechanical
Average Peak Threshold (grams)
15
10
5
0
n.Vehicle
n.AP
E.
Group III/IV
Mechanical Sensitization
Peak Firing Rate (Hz)
Pre/Post Metabolite Treatment
20
15
10
5
0
*
Pre-
Post-
Pre-
Post-
F.
Group III/IV
Mechanical
Average Firing Rate
(Hz)
6
4
2
0
0.07
0.4
1
2
4
10
Force applied
(grams)
*
n.Vehicle
n.AP
G.
Group III/IV
Proportions
Percent Responders
80
60
40
20
0
*
#
Mechanical
Thermal - Cold
Thermal - Hot
Chemical - Low
Chemical - High
Chemical - Both
Silent

Figure 3

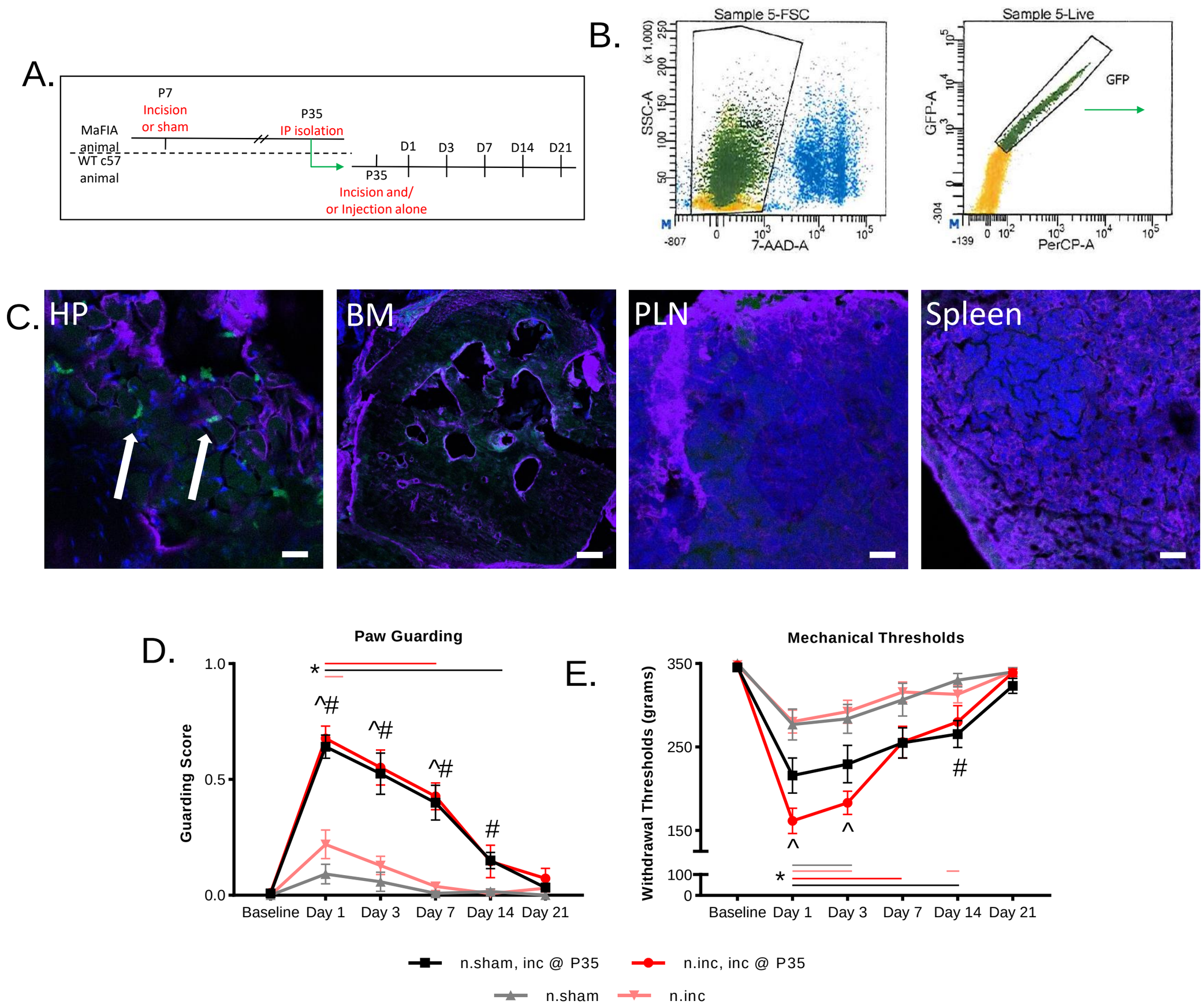
A.
P7
Incision
or sham
P35
IP isolation
MaFIA
animal
WT c57
animal
D1
D3
D7
D14
D21
P35
Incision and/
or Injection alone
B.
Sample 5-FSC
SSC-A
7-AAD-A
Live
Sample 5-Live
GFP-A
PerCP-A
GFP
C.
HP
BM
PLN
Spleen
D.
Paw Guarding
Guarding Score
Baseline
Day 1
Day 3
Day 7
Day 14
Day 21
E.
Mechanical Thresholds
Withdrawal Thresholds (grams)
n.sham, inc @ P35
n.inc, inc @ P35
n.sham
n.inc

Figure 4

A.

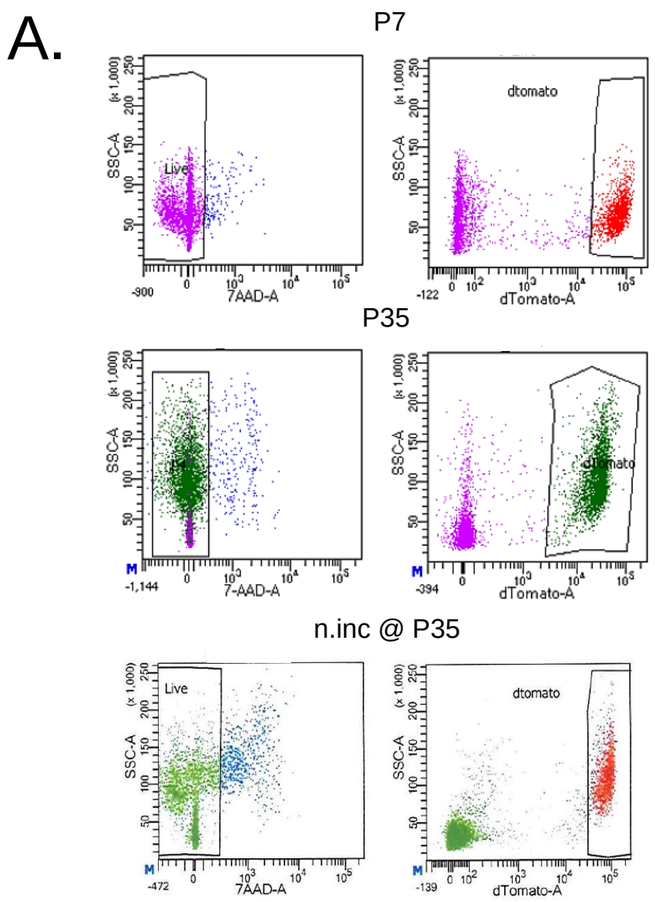

B.

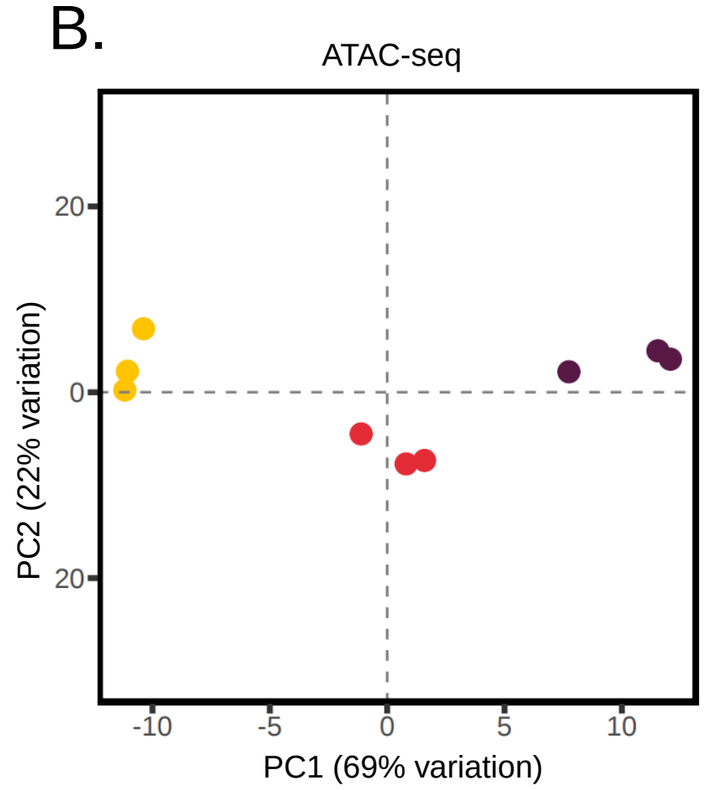

C.

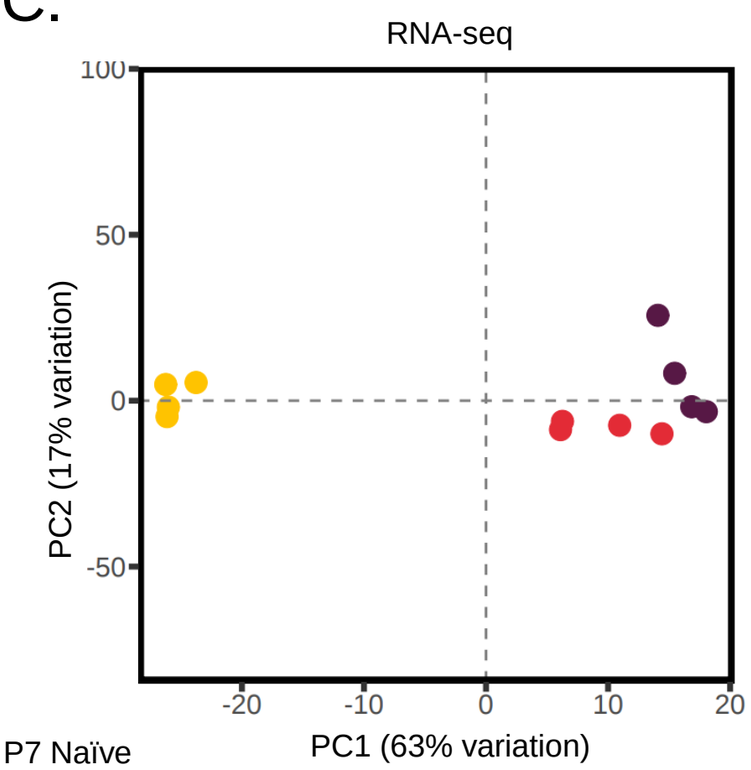

P7 Naïve
P35 Naïve
P7 inc. @ P35

D.

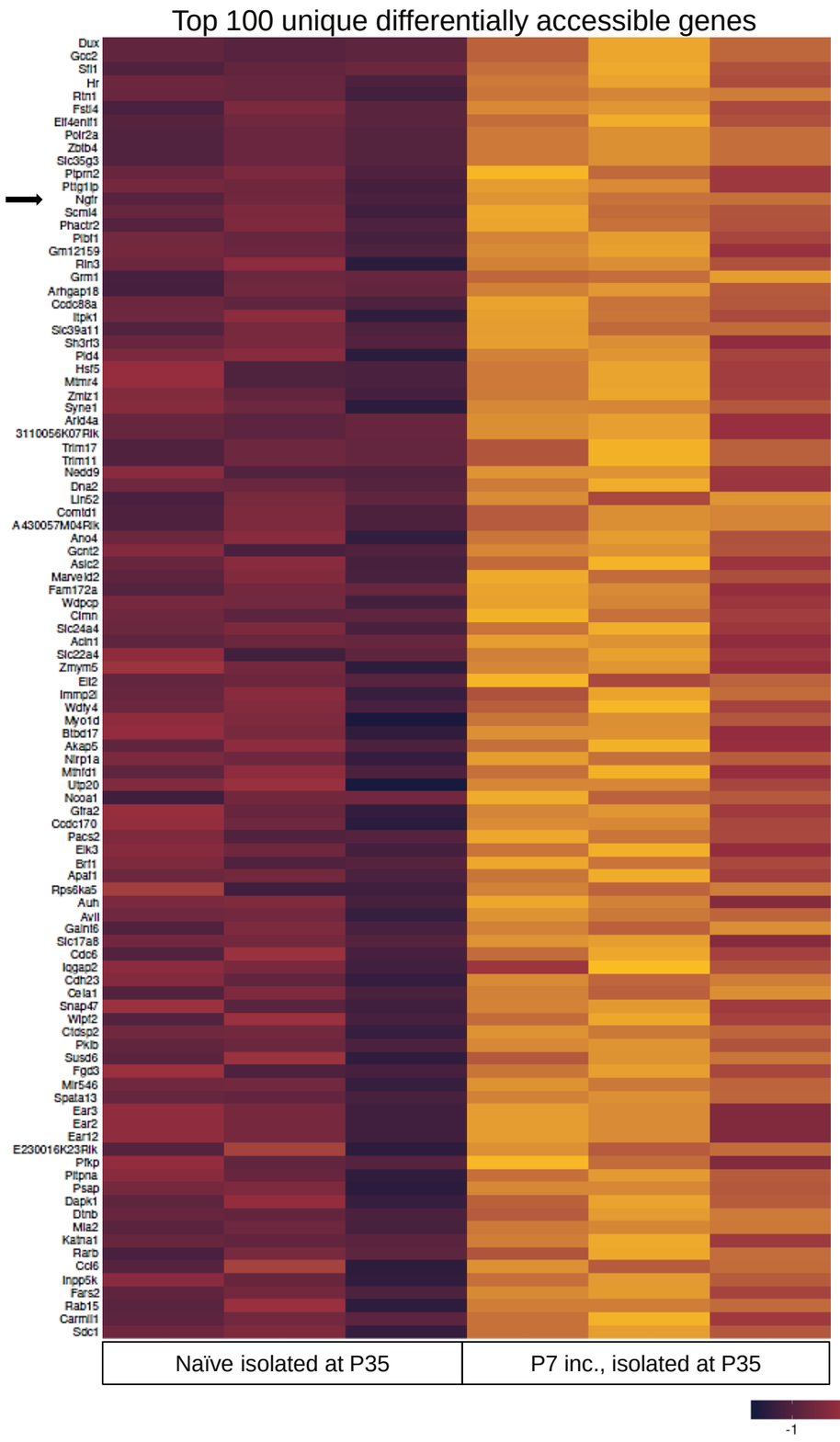

E.

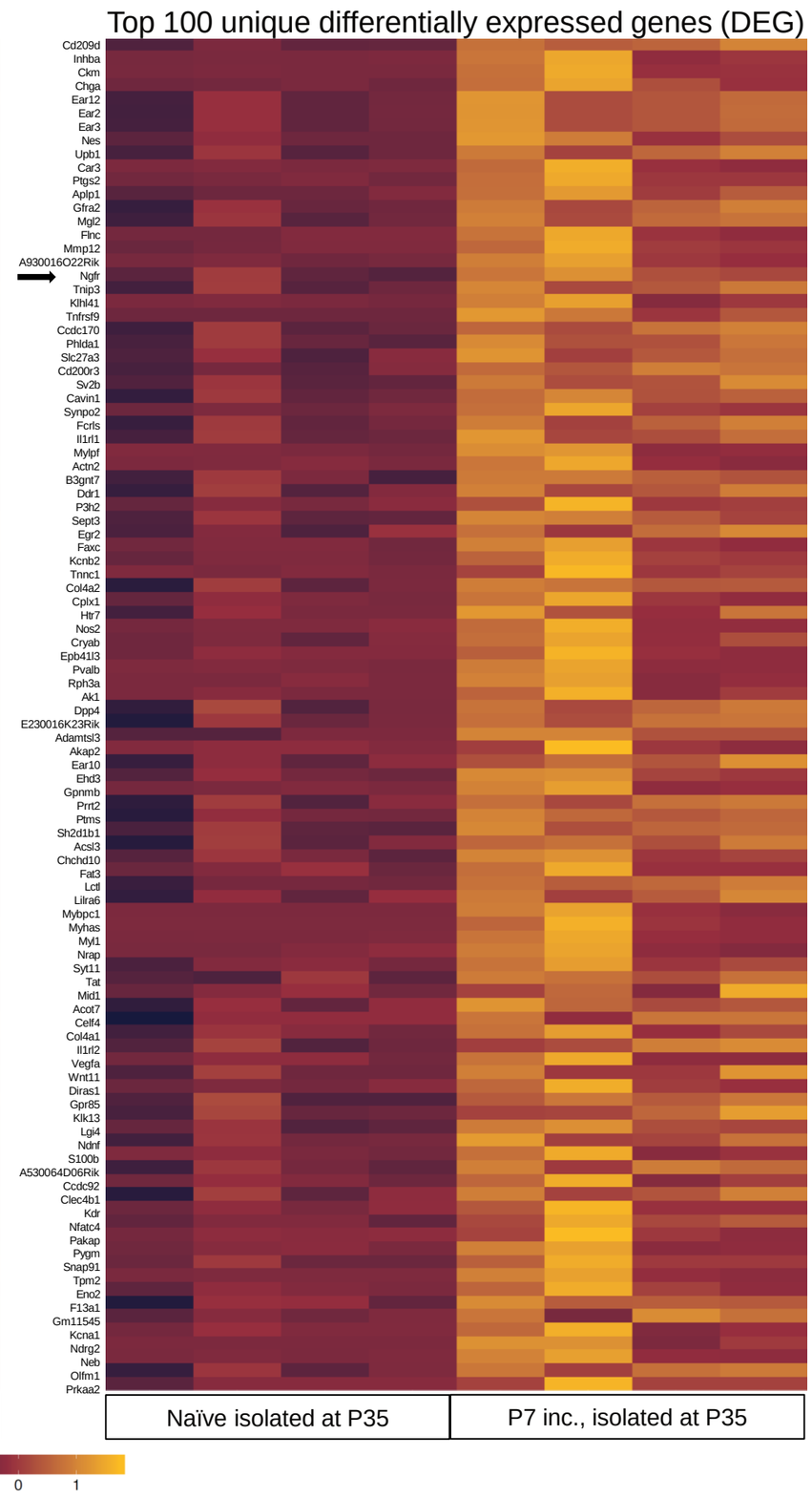

F.

DEGs that agree with accessible genes:

Up			
Hr	Klrb1a	Rtn1	Magi2
Ngfr	Ppp1r16b	Celf4	Mras
Gsn	Pvalb		
Down			
Mfap4			

G.

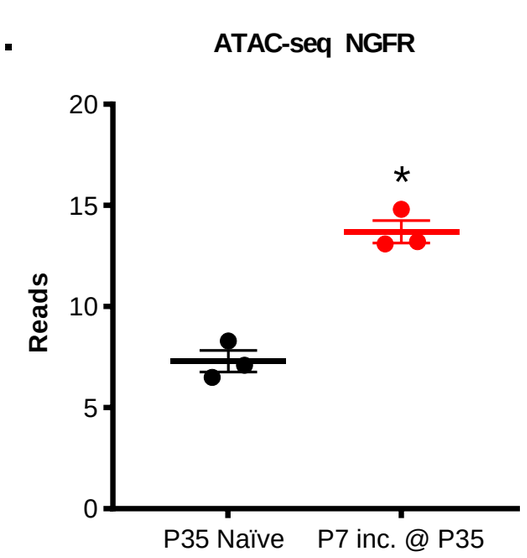

H.

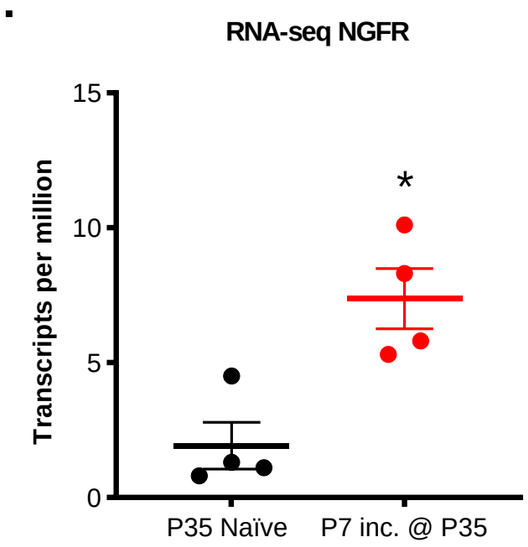

Figure 5

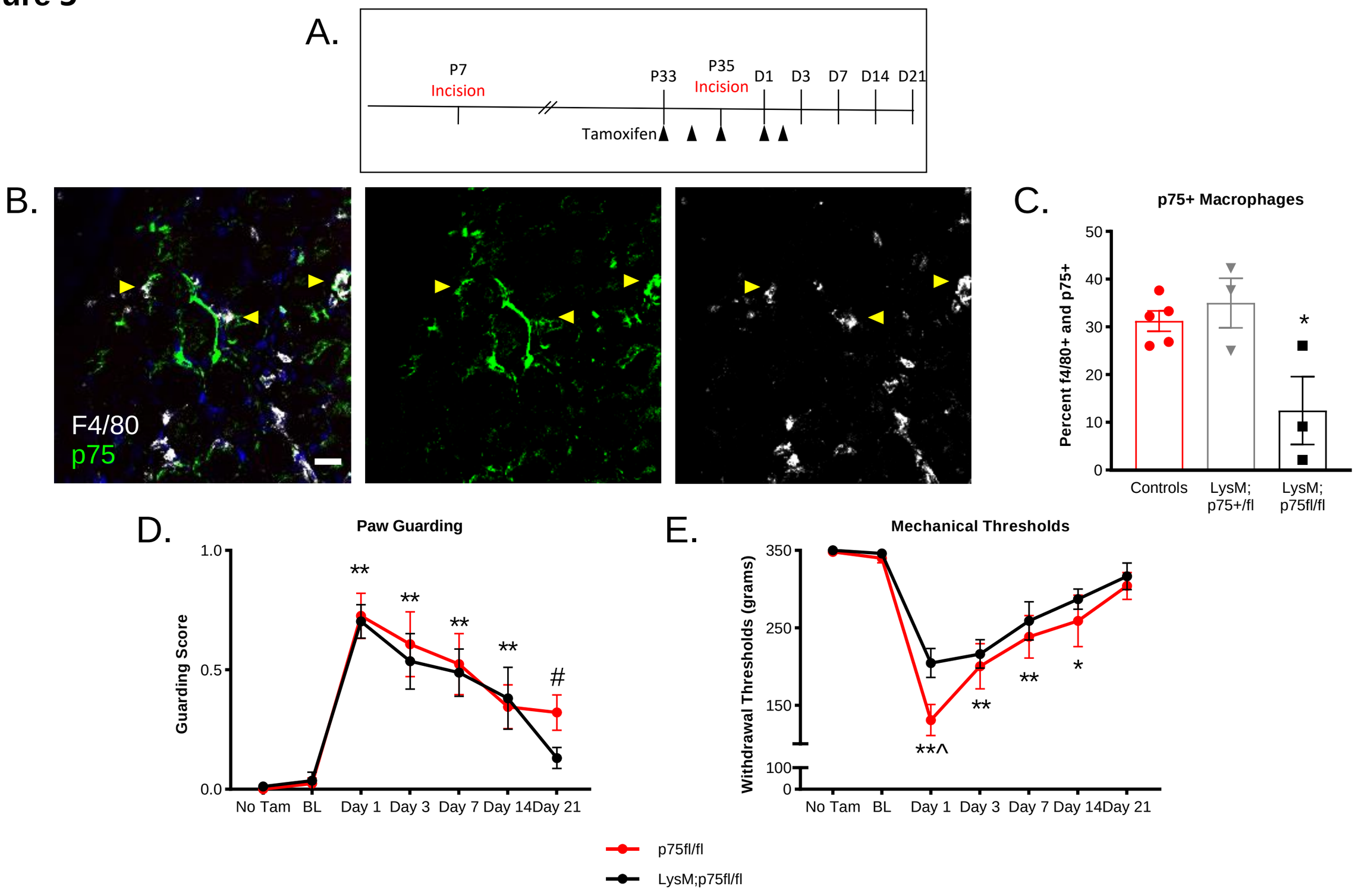
A.
P7
Incision
P33
P35
Incision
D1
D3
D7
D14
D21
Tamoxifen
B.
F4/80
p75
C.
p75+ Macrophages
Percent f4/80+ and p75+
50
40
30
20
10
0
*
Controls
LysM; p75+/fl
LysM; p75fl/fl
D.
Paw Guarding
Guarding Score
1.0
0.5
0.0
**
**
**
**
#
No Tam
BL
Day 1
Day 3
Day 7
Day 14
Day 21
E.
Mechanical Thresholds
Withdrawal Thresholds (grams)
350
250
150
100
0
**^
**
**
*
No Tam
BL
Day 1
Day 3
Day 7
Day 14
Day 21
p75fl/fl
LysM;p75fl/fl

Figure 6

A.

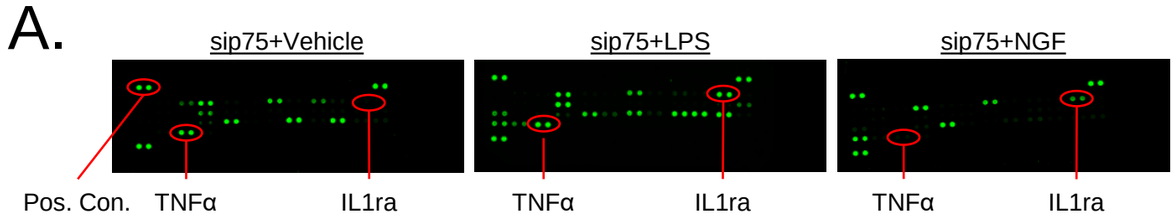

B.

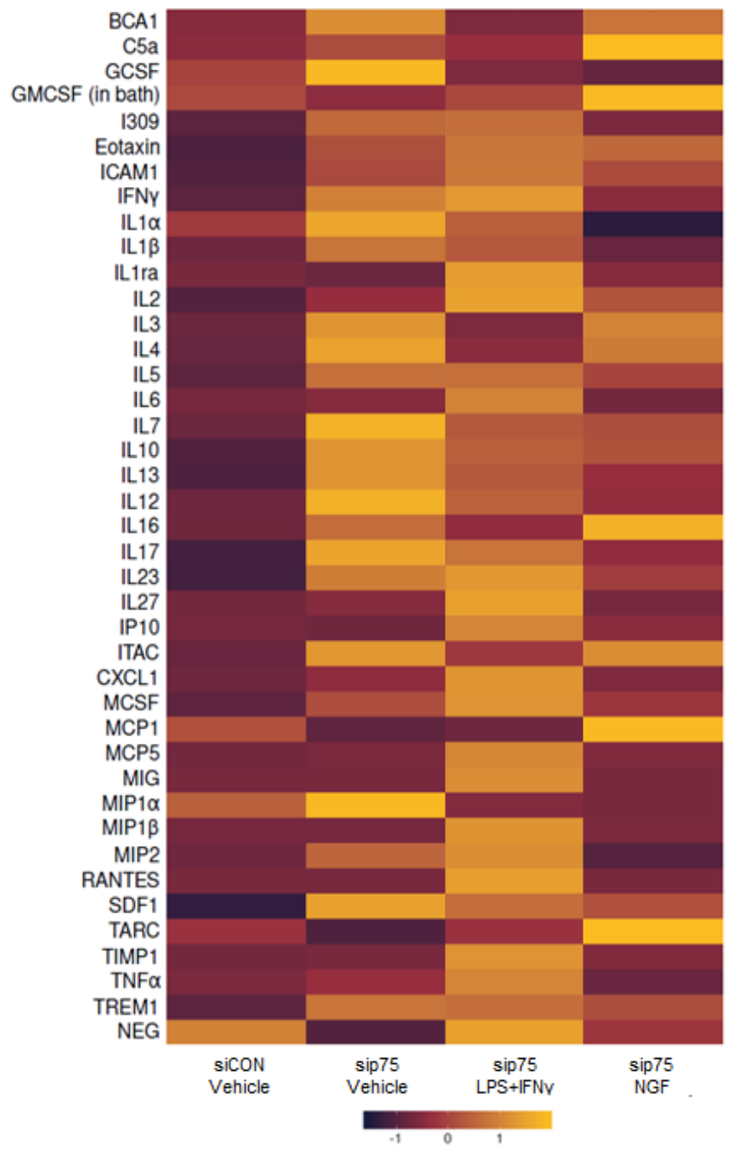

C.

% Change from siCON+Vehicle			
Protein	**sip75+Veh**	**sip75+LPS**	**sip75+NGF**
TNFα	572 ± 469%	8392 ± 5043%*	24 ± 54%^
IL1β	253 ± 153%	322 ± 154%	34 ± 39%#
IL1α	-68 ± 14%	24 ± 88%	-78 ± 16%
IL6	1036 ± 920%	19944 ± 9191%*	31 ± 44%
IL1ra	-31 ± 36%	4104 ± 3619%	193 ± 189%
IFNγ	76 ± 10%*	177 ± 39%*	14 ± 16%
IL4	140 ± 133%	35 ± 14%	98 ± 33%*
IL10	91 ± 30%*	113 ± 38%	57 ± 33%##

D.

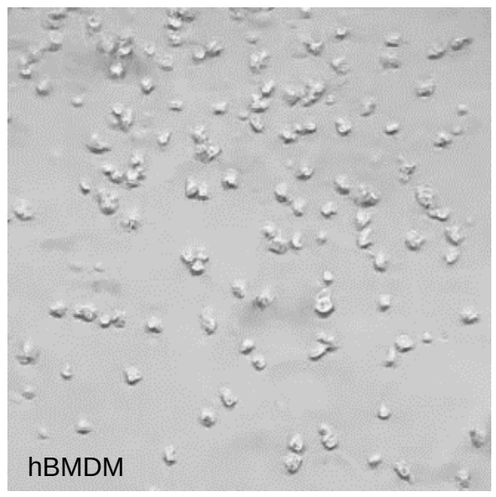

E.

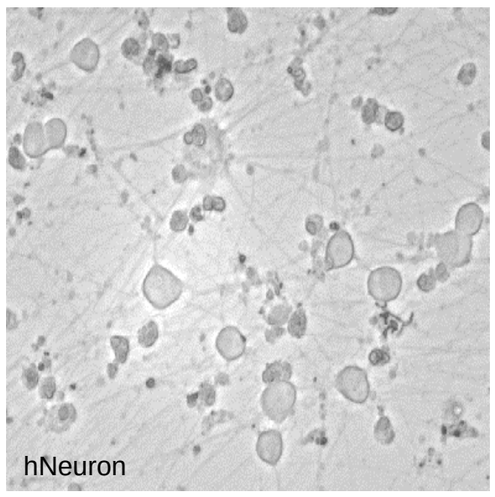

F.

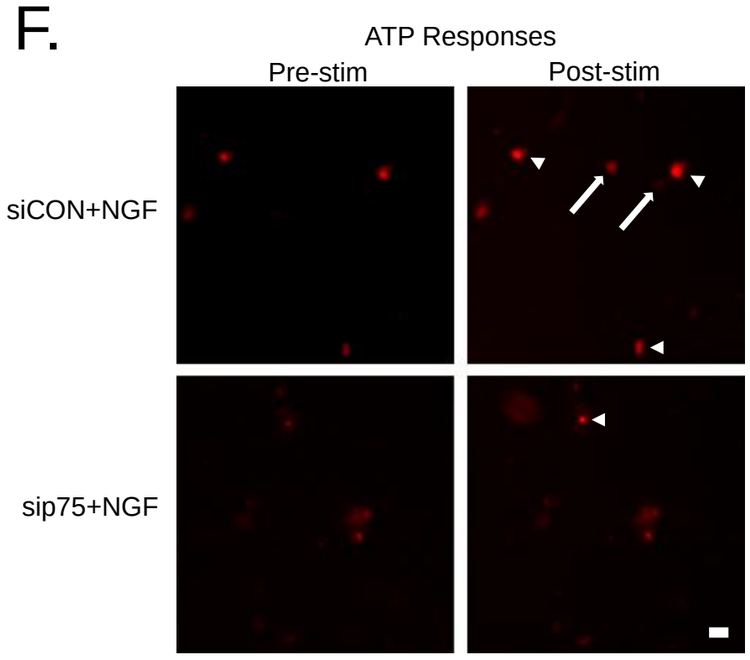

G.

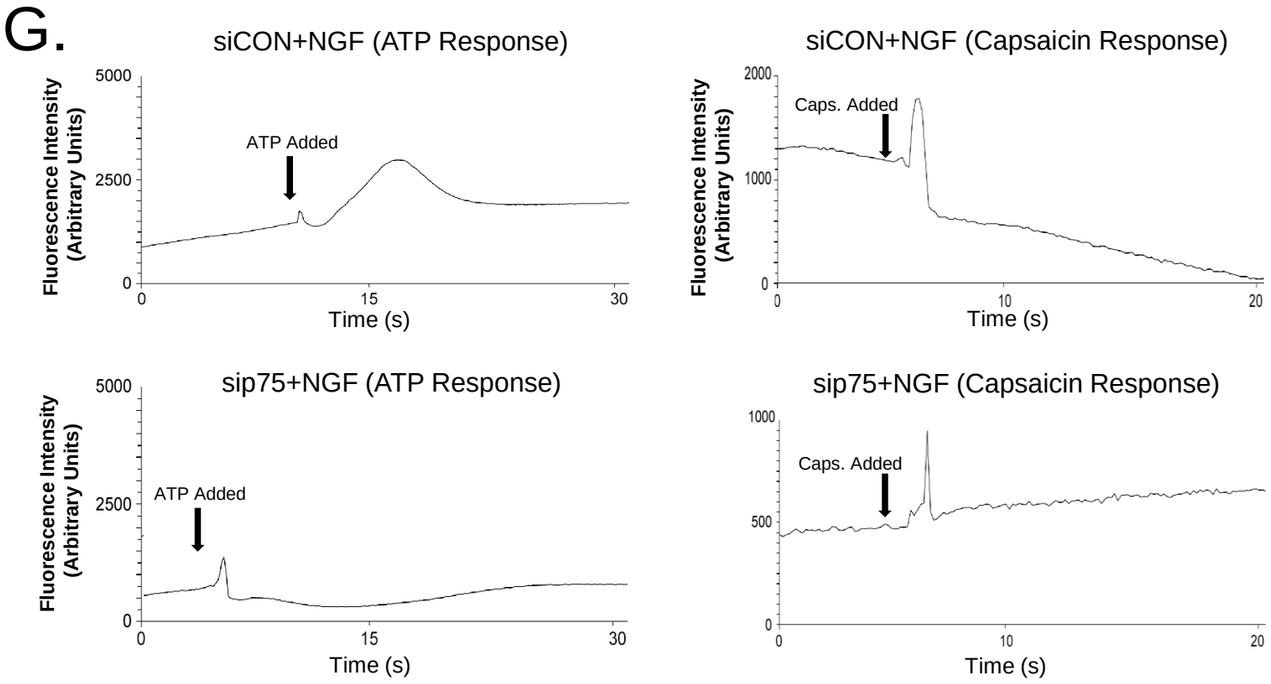

H.

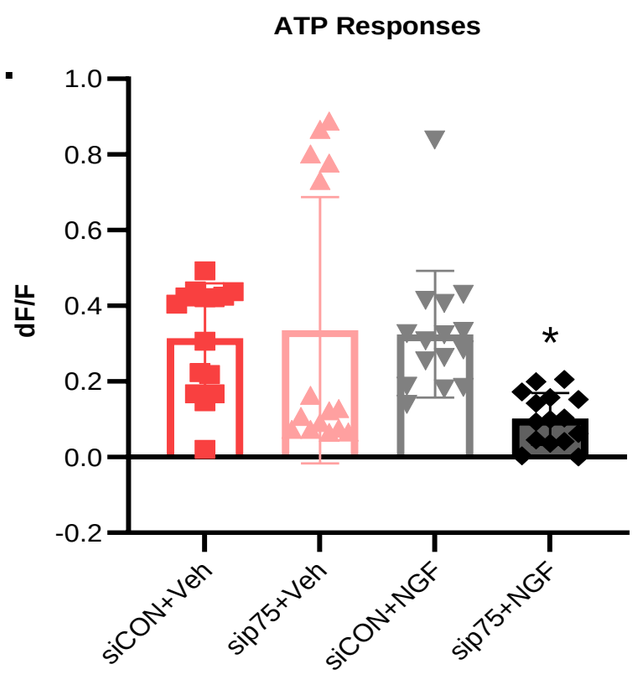

I.

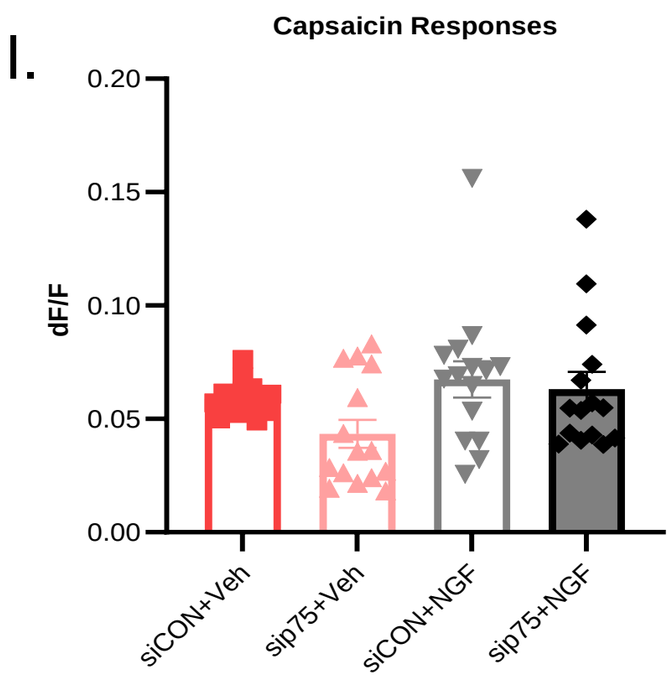

Figure 7

A.

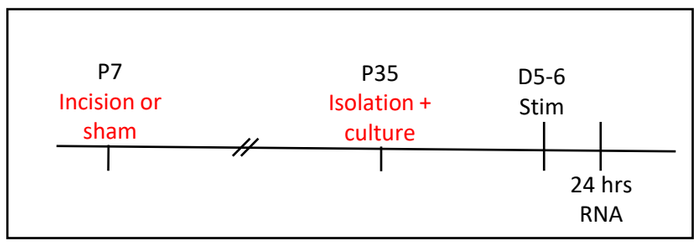

B.

% Change Macrophage mRNA

Gene	n.sham stim'd	n.inc stim'd
IL1b	78 ± 16 %	255 ± 20 %*^
IL6	-80 ± 101 %	-84 ± 103 %*
TNFa	117 ± 26 %	76 ± 25 %
IL10	-48 ± 52 %	-52 ± 83 %
ARG1	-63 ± 28 %	-91 ± 44 %*^

C.

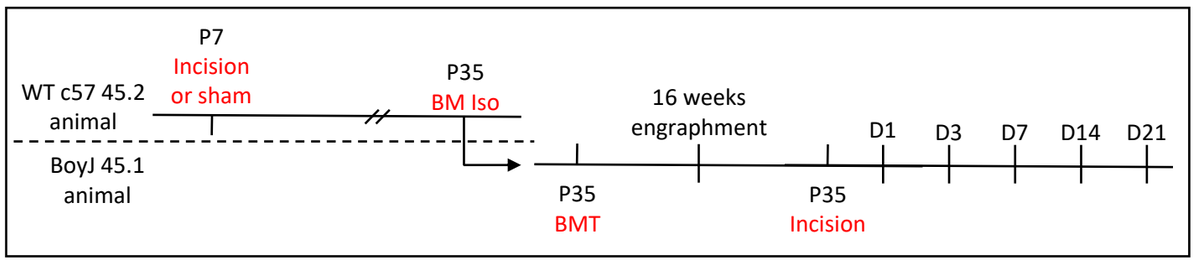

D.

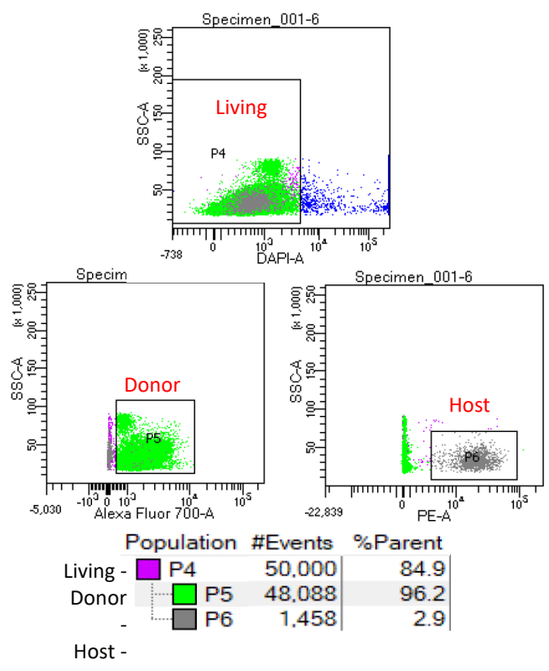

E.

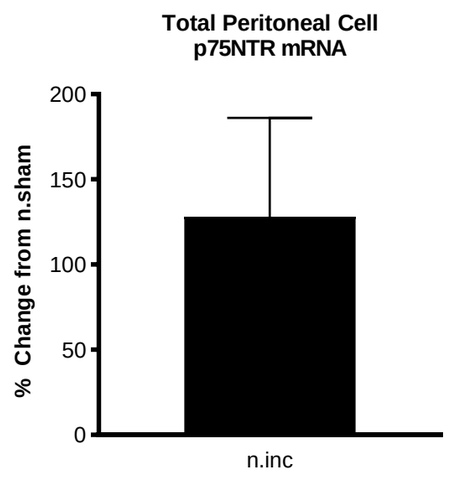

F.

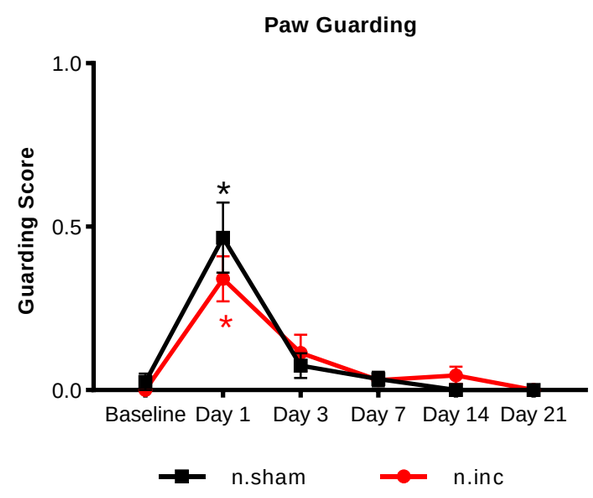

G.

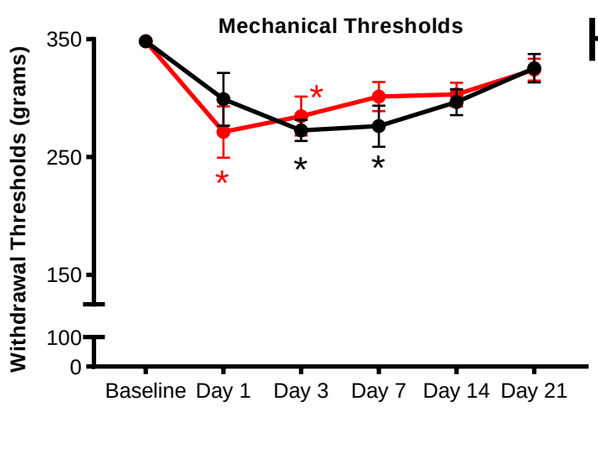

H.

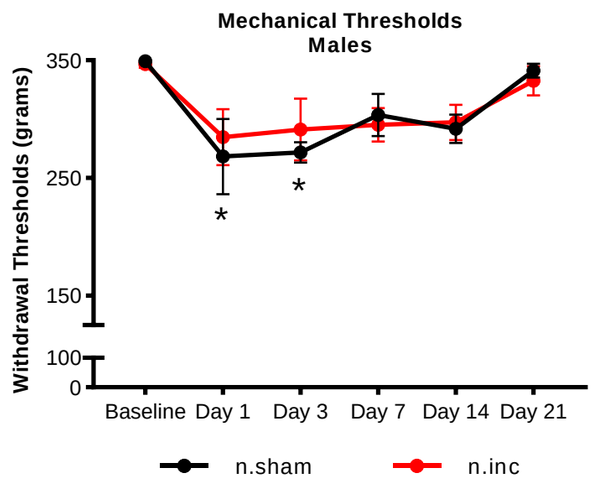

I.

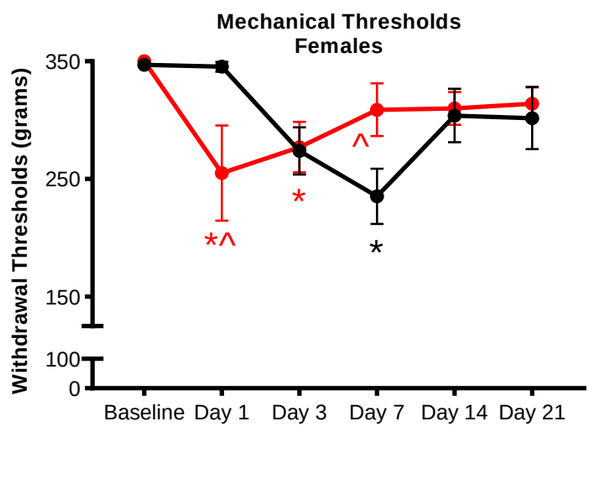

Graphical Abstract

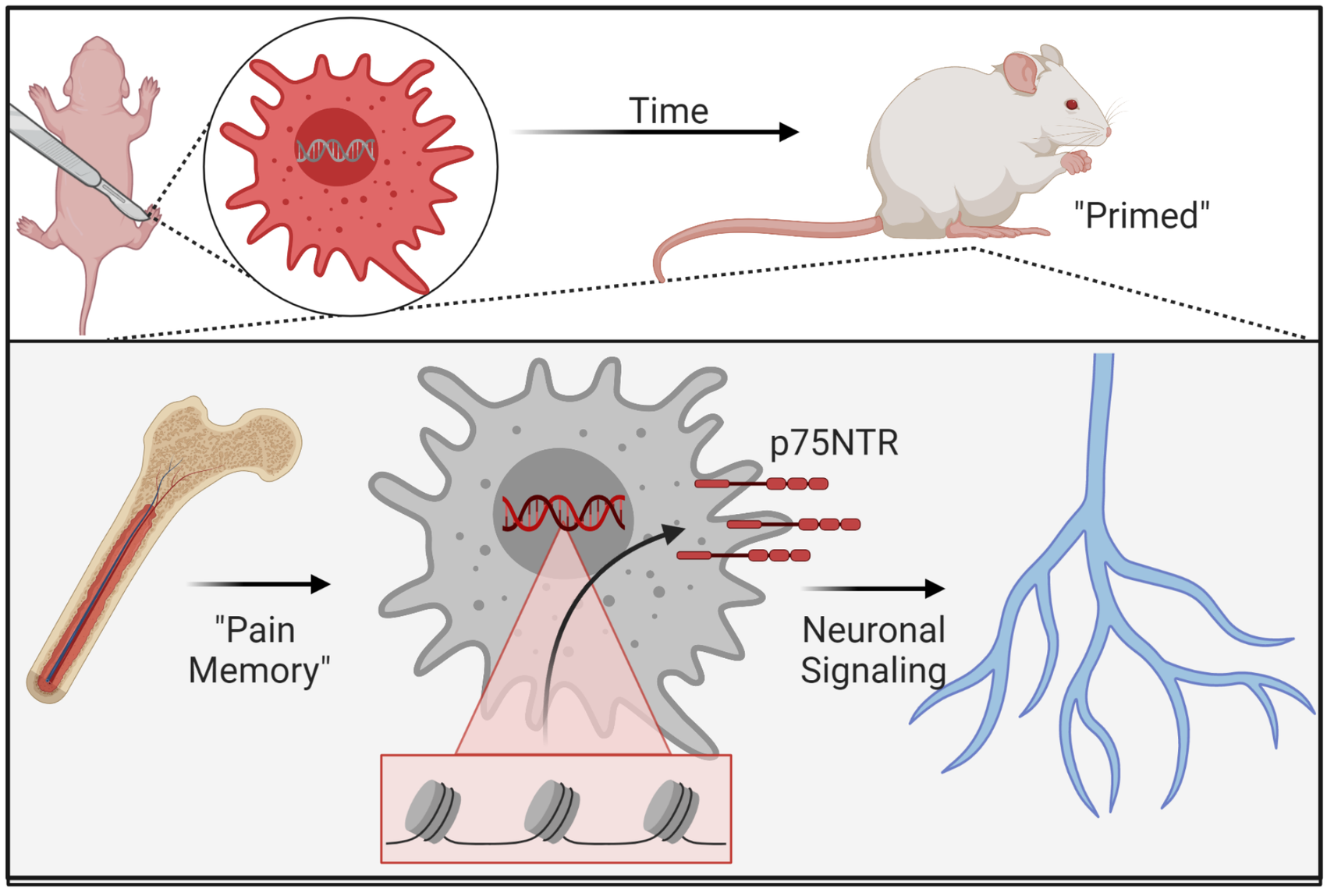

Supplemental Figure 1

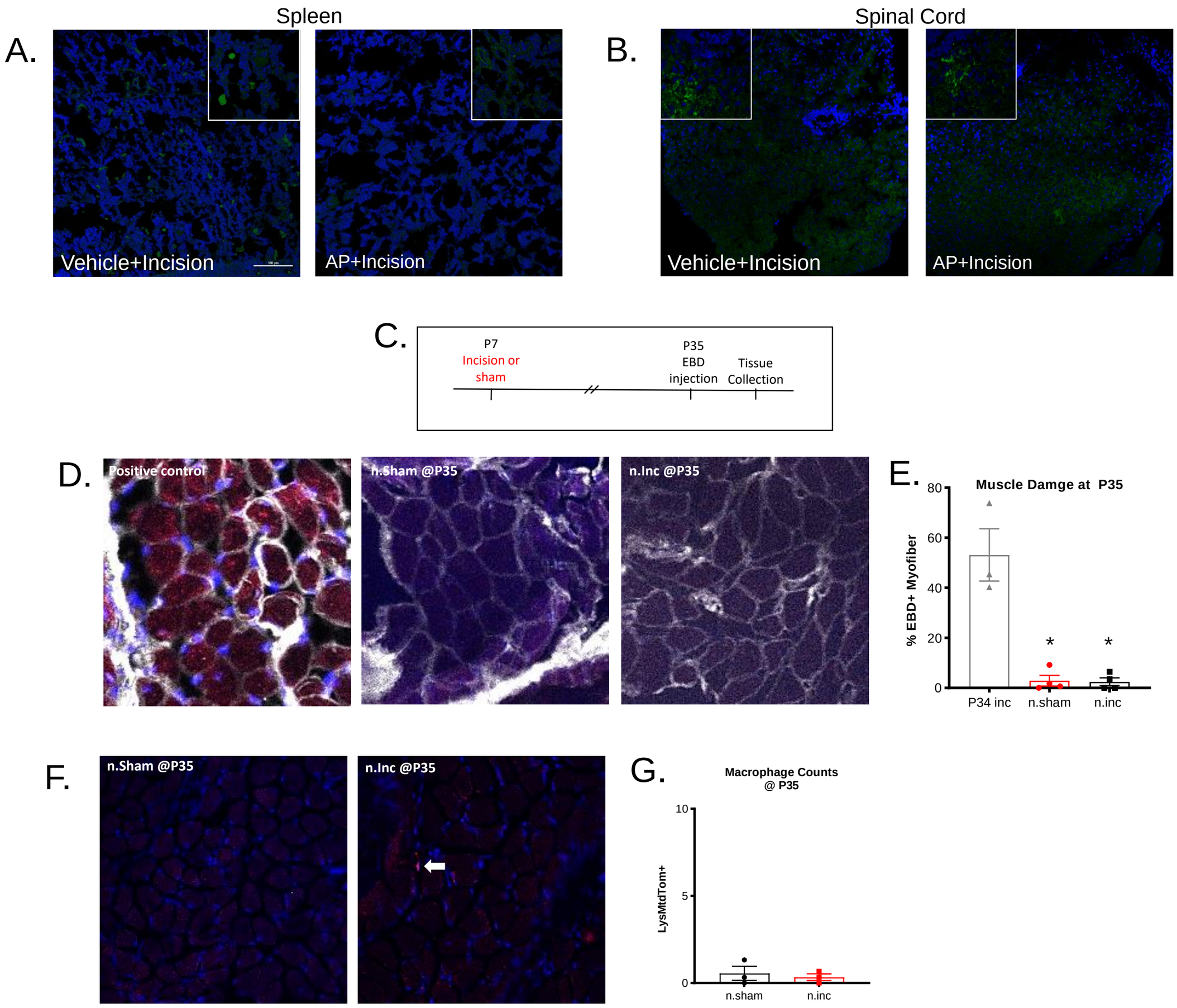

Supplemental Figure 2

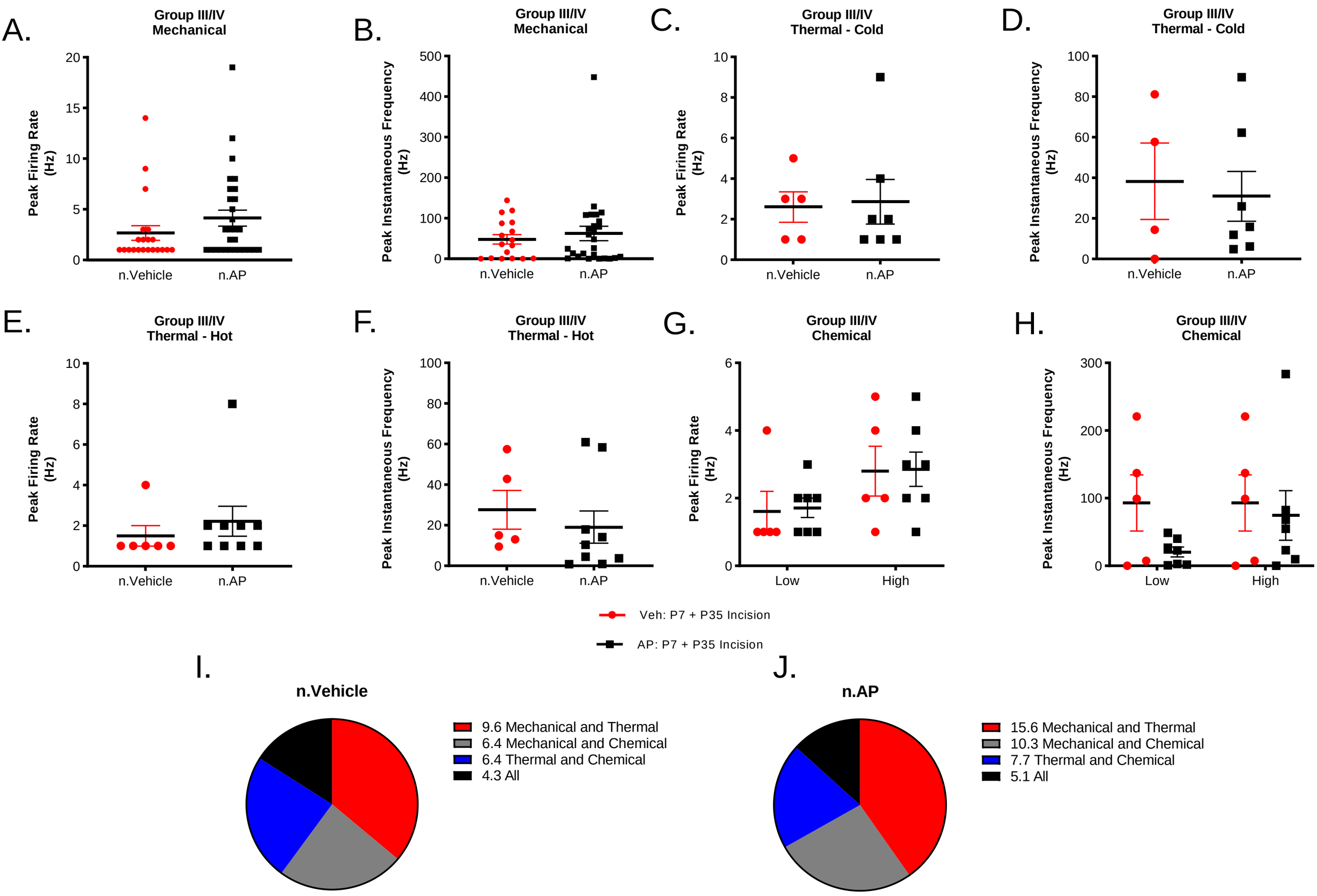

Supplemental Figure 3

A.

Condition	ATAC-seq peak count	Most similar cell type (public data)	Most similar molecule (public data)
P7 Naïve Isolation	76,624	BMDM_macrophages	Pu1
P7 Naïve Isolation	80,621	BMDM_macrophages	Pu1
P7 Naïve Isolation	58,325	BMDM_macrophages	Pu1
P35 Naïve Isolation	75,182	BMDM_macrophages	Pu1
P35 Naïve Isolation	76,673	macrophage	Pu1
P35 Naïve Isolation	74,305	macrophage	Pu1
P7 Incised, P35 Isolation	57,259	macrophage	Pu1
P7 Incised, P35 Isolation	56,885	Macrophage	Pu1
P7 Incised, P35 Isolation	69,108	BMDM_macrophages	Pu1

B.

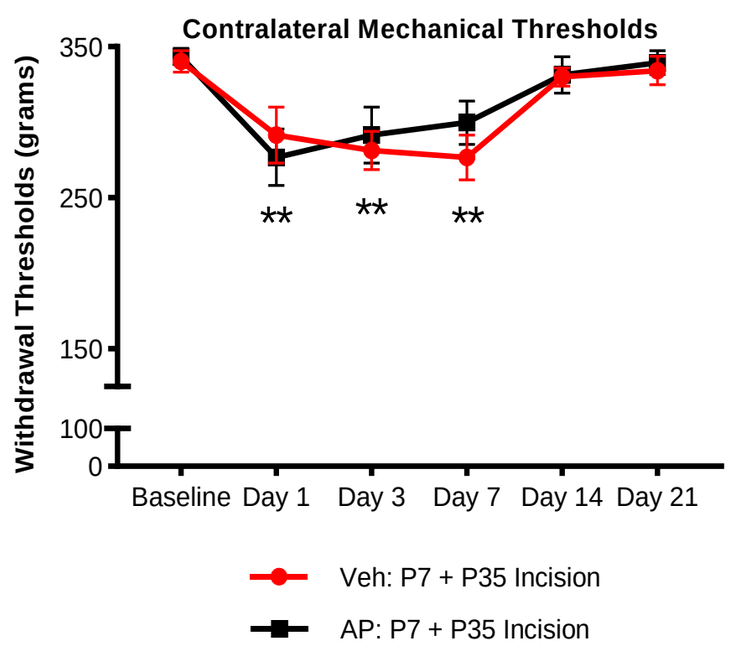

C.

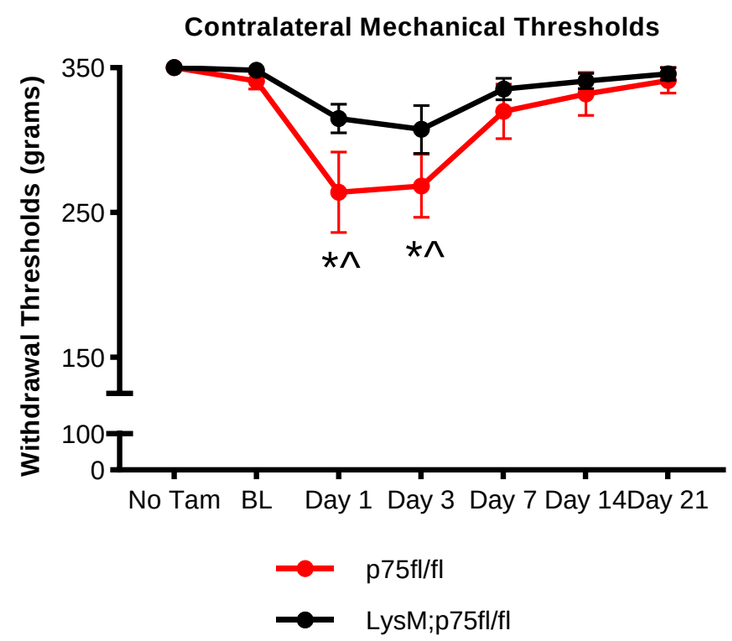

Supplemental Figure

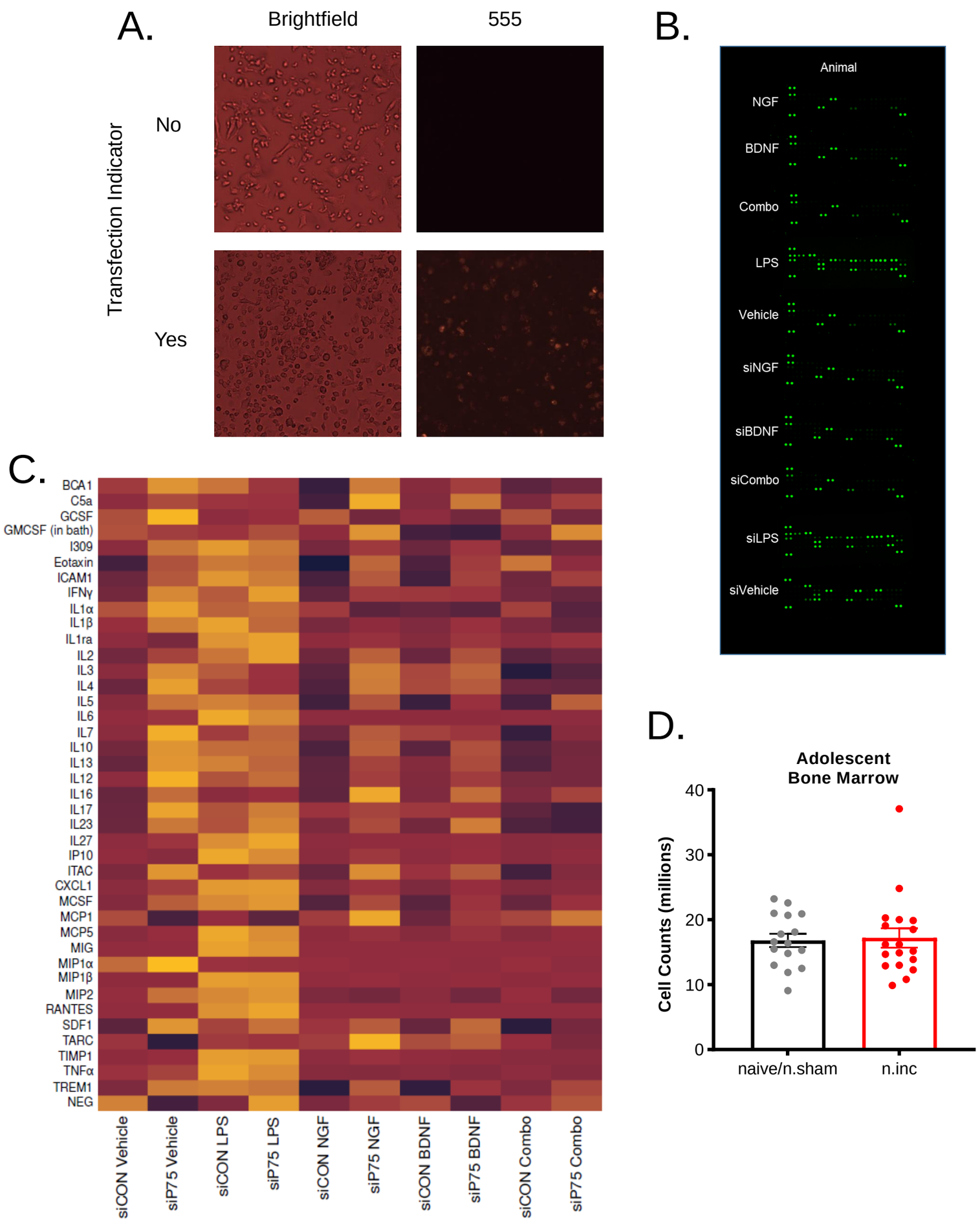

Supplemental Table

	% Change from siCON+Vehicle								
Protein	**sip75+Veh**	**siCON+LPS**	**sip75+LPS**	**siCON+NGF**	**sip75+NGF**	**siCON+BDNF**	**sip75+BDNF**	**siCON+Combo**	**sip75+Combo**
BCA1	10 ± 17 %	47 ± 13 %	0 ± 10 %	-20 ± 4 %	11 ± 14 %	-7 ± 9 %	-13 ± 6 %	-7 ± 11 %	-24 ± -24 %
C5a	12 ± 15 %	32 ± 21 %	19 ± 17 %	-43 ± 4 %	160 ± 72 %	-2 ± 11 %	95 ± 45 %	1 ± 20 %	18 ± 18 %
GCSF	1258 ± 733 %	136 ± 112 %	290 ± 164 %	18 ± 11 %	30 ± 54 %	0 ± 27 %	14 ± 40 %	4 ± 3 %	27 ± 27 %
GMCSF	-18 ± 26 %	36 ± 51 %	30 ± 42 %	5 ± 26 %	31 ± 33 %	-26 ± 11 %	-41 ± 7 %	7 ± 29 %	30 ± 30 %
I309	127 ± 66 %	482 ± 284 %	252 ± 116 %	8 ± 24 %	37 ± 42 %	-7 ± 23 %	33 ± 37 %	-12 ± 20 %	-13 ± -13 %
Eotaxin	57 ± 33 %	219 ± 65 %	189 ± 53 %	-18 ± 6 %	105 ± 18 %	14 ± 15 %	59 ± 18 %	217 ± 62 %	27 ± 27 %
ICAM1	58 ± 49 %	286 ± 162 %	199 ± 66 %	-16 ± 15 %	76 ± 48 %	-20 ± 41 %	44 ± 43 %	24 ± 32 %	43 ± 43 %
IFNy	76 ± 10 %	158 ± 31 %	177 ± 39 %	-1 ± 14 %	14 ± 16 %	36 ± 13 %	9 ± 14 %	14 ± 9 %	-17 ± -17 %
IL1a	575 ± 472 %	665 ± 437 %	427 ± 176 %	4 ± 34 %	-15 ± 38 %	-15 ± 46 %	-16 ± 40 %	2 ± 27 %	-25 ± -25 %
IL1b	253 ± 153 %	734 ± 575 %	322 ± 154 %	2 ± 21 %	34 ± 39 %	12 ± 29 %	53 ± 48 %	21 ± 27 %	-25 ± -25 %
IL1ra	-31 ± 36 %	669 ± 167 %	4104 ± 3619 %	30 ± 16 %	193 ± 189 %	5 ± 30 %	240 ± 216 %	5 ± 12 %	245 ± 245 %
IL2	29 ± 10 %	243 ± 86 %	295 ± 84 %	7 ± 20 %	102 ± 26 %	-4 ± 10 %	84 ± 34 %	-9 ± 9 %	-15 ± -15 %
IL3	11 ± 16 %	40 ± 7 %	7 ± 7 %	0 ± 12 %	17 ± 3 %	19 ± 14 %	8 ± 14 %	-7 ± 11 %	-20 ± -20 %
IL4	140 ± 133 %	63 ± 16 %	35 ± 14 %	-6 ± 9 %	98 ± 33 %	76 ± 69 %	60 ± 20 %	17 ± 20 %	-12 ± -12 %
IL5	28 ± 15 %	136 ± 75 %	103 ± 60 %	-15 ± 14 %	31 ± 31 %	-16 ± 18 %	1 ± 20 %	-13 ± 11 %	56 ± 56 %
IL6	1036 ± 920 %	35132 ± 18092 %	19944 ± 9191 %	-52 ± 14 %	31 ± 44 %	-23 ± 20 %	112 ± 128 %	65 ± 69 %	13 ± 13 %
IL7	31 ± 13 %	28 ± 30 %	37 ± 4 %	3 ± 15 %	13 ± 24 %	28 ± 30 %	-7 ± 12 %	-7 ± 13 %	-8 ± -8 %
IL10	91 ± 30 %	148 ± 75 %	113 ± 38 %	-8 ± 15 %	57 ± 33 %	-1 ± 21 %	42 ± 23 %	2 ± 16 %	-6 ± -6 %
IL13	62 ± 25 %	128 ± 74 %	86 ± 31 %	14 ± 23 %	22 ± 22 %	24 ± 22 %	30 ± 21 %	9 ± 17 %	-3 ± -3 %
IL12	92 ± 36 %	70 ± 50 %	96 ± 36 %	-7 ± 23 %	9 ± 19 %	3 ± 19 %	7 ± 16 %	5 ± 13 %	-19 ± -19 %
IL16	15 ± 25 %	49 ± 50 %	21 ± 19 %	23 ± 32 %	63 ± 47 %	23 ± 47 %	40 ± 52 %	36 ± 38 %	16 ± 16 %
IL17	93 ± 56 %	108 ± 79 %	110 ± 29 %	48 ± 34 %	27 ± 27 %	45 ± 35 %	17 ± 29 %	12 ± 14 %	-20 ± -20 %
IL23	35 ± 17 %	64 ± 24 %	116 ± 24 %	21 ± 19 %	20 ± 12 %	6 ± 2 %	69 ± 24 %	3 ± 17 %	-24 ± -24 %
IL27	67 ± 22 %	1327 ± 627 %	1556 ± 336 %	17 ± 15 %	0 ± 7 %	25 ± 16 %	20 ± 3 %	-2 ± 6 %	-21 ± -21 %
IP10	-45 ± 22 %	1977 ± 118 %	2556 ± 1661 %	3 ± 17 %	202 ± 132 %	8 ± 15 %	112 ± 124 %	-22 ± 6 %	61 ± 61 %
ITAC	34 ± 28 %	23 ± 17 %	29 ± 19 %	4 ± 16 %	43 ± 9 %	16 ± 18 %	17 ± 4 %	-4 ± 11 %	-10 ± -10 %
CXCL1	48 ± 22 %	794 ± 388 %	660 ± 232 %	-4 ± 17 %	33 ± 24 %	-19 ± 12 %	10 ± 17 %	-3 ± 18 %	-9 ± -9 %
MSCF	35 ± 32 %	207 ± 102 %	183 ± 72 %	-13 ± 16 %	32 ± 25 %	-12 ± 17 %	9 ± 27 %	2 ± 17 %	10 ± 10 %
MCP1	-35 ± 27 %	31 ± 32 %	-16 ± 27 %	9 ± 17 %	37 ± 12 %	-20 ± 15 %	-13 ± 17 %	18 ± 26 %	25 ± 25 %
MCP5	36 ± 29 %	2115 ± 925 %	1624 ± 481 %	41 ± 4 %	75 ± 9 %	-13 ± 11 %	82 ± 17 %	-3 ± 13 %	39 ± 39 %
MIG	37 ± 24 %	13556 ± 6039 %	10033 ± 2898 %	13 ± 22 %	21 ± 19 %	8 ± 22 %	10 ± 13 %	6 ± 13 %	-18 ± -18 %
MIP1a	1670 ± 1601 %	165 ± 144 %	85 ± 73 %	-9 ± 31 %	8 ± 37 %	-18 ± 27 %	-14 ± 29 %	-6 ± 29 %	-20 ± -20 %
MIP1b	-9 ± 31 %	7235 ± 2620 %	8906 ± 4543 %	79 ± 35 %	129 ± 55 %	34 ± 25 %	105 ± 71 %	5 ± 5 %	88 ± 88 %
MIP2	4924 ± 3763 %	14064 ± 7228 %	11931 ± 4206 %	18 ± 37 %	10 ± 37 %	24 ± 23 %	-6 ± 32 %	42 ± 19 %	-19 ± -19 %
RANTES	59 ± 31 %	11986 ± 3798 %	12424 ± 1735 %	19 ± 16 %	1 ± 19 %	-24 ± 13 %	9 ± 19 %	31 ± 10 %	3 ± 3 %
SDF1	42 ± 20 %	50 ± 5 %	66 ± 25 %	34 ± 13 %	25 ± 5 %	8 ± 9 %	38 ± 7 %	-2 ± 4 %	-5 ± -5 %
TARC	-56 ± 25 %	4194 ± 4177 %	4434 ± 4455 %	3034 ± 3026 %	6719 ± 6648 %	4422 ± 4411 %	4978 ± 4979 %	1351 ± 1351 %	1934 ± 1934 %
TIMP1	-6 ± 10 %	1159 ± 345 %	1097 ± 305 %	7 ± 15 %	42 ± 11 %	16 ± 8 %	-9 ± 12 %	-3 ± 15 %	-25 ± -25 %
TNFa	572 ± 469 %	13303 ± 7767 %	8392 ± 5043 %	0 ± 50 %	24 ± 54 %	-28 ± 21 %	-30 ± 29 %	2 ± 32 %	-26 ± -26 %
TREM1	34 ± 30 %	137 ± 90 %	88 ± 39 %	-12 ± 19 %	33 ± 32 %	-11 ± 23 %	10 ± 36 %	21 ± 17 %	34 ± 34 %

Supplemental Figure 1. No persistent effects of early life incision are found on muscle integrity.

A. Representative images from the spleen at P8 after treatment with either vehicle or AP in MaFIA animals indicating a loss of GFP+ cells in the AP treated group. **B.** Images of the spinal cord of the same animals indicating continued expression of GFP in both groups. **C.** Experimental design for the collection of tissue in D-G. **D.** Representative images of EBD (red) counter stained with WGA (white) and DAPI (blue) in acutely injured tissue compared to latent changes four weeks after an early life incision or sham. **E.** In tissue damaged two days before dissection, there is robust EBD leakage into myofibers that is absent in neonatal injured myofibers (*$p<0.001$ vs. P34 inc., One-way ANOVA, Tukey's, n=3-4/group). **F.** Images indicating LysM+ myeloid cells (tdTomato reporter) in adolescent tissue from neonatal injured or sham animals. **G.** There is no difference in the number of macrophages present in the muscle in neonatal incised animals compared to sham operated animals ($p=0.643$ n.inc vs. n.sham, One-way ANOVA, Tukey's, n=3/group). Data shown as mean +/- SEM.

Supplemental Figure 2. Additional electrophysiological properties of DRG neurons after repeated surgical injury.

A-B. There is no change in mechanical firing rate (A, $p=0.135$) nor instantaneous frequency (B, $p=0.804$) between groups. **C-D.** Firing rates and instantaneous frequencies of cold responders is not different between groups (FR: $p=0.876$, IF: $p=0.738$, n.AP vs. n.Vehicle, n=7 and 5 respectively, ANOVA on Ranks, Dunn's). **E-F.** There are no differences in heat responders between groups (FR: $p=0.226$, IF: $p=0.386$, n.AP vs. n.Vehicle, n=9 and 6 respectively, ANOVA on Ranks, Dunn's). **G-H.** There is no difference in the firing rate nor instantaneous frequencies of chemically sensitive cells (Low: FR: $p=0.530$, IF: $p=0.343$, n.AP vs. n.Vehicle, n=7 and 5

respectively, ANOVA on Ranks, Dunn's, High: FR: p=0.948, IF: 0.748, n.AP vs. n.Vehicle, n=7 and 5 respectively, ANOVA on Ranks, Dunn's). **I-J.** There is no change in the proportion of polymodal responders between groups (n.AP vs. n.Vehicle, Chi-square or Fisher's Exact). Data shown as mean +/- SEM.

Supplemental Figure 3. ATAC-seq quality control and the effect of dual incision on contralateral mechanical withdrawal thresholds.

A. Quality control analyses reveal a pure population of cells that are likely macrophages based on open chromatin regions and previous sequencing datasets. **B.** Animals that received dual incision regardless of treatment with AP or vehicle had a significant reduction of contralateral mechanical withdrawal thresholds (F=15.337) that lasted for at least seven days (**p<0.05 vs. BL, both groups, Two-way RM ANOVA, Tukey's, n=10-12. **C.** Contralateral muscle squeezing is affected by the knockout of p75NTR in LysM+ cells following dual incision (F=13.047) on days one and three (*p<0.001 vs. p75fl/fl BL, ^p<0.05 vs. LysM;p75fl/fl, Two-way RM ANOVA, Tukey's, n=7/group). Data shown as mean +/- SEM.

Supplemental Figure 4: Transfection efficiency and regulation of bone marrow derived macrophages.

A. Example pictures of the transfection efficiency to knockdown p75NTR in BMDMs. **B.** Example blots macrophages that were treated with different stimulants and the knockdown of p75NTR. **C.** A heatmap consisting of all manipulations for the 40 proteins included in the arrays. **D.** An analysis indicating no difference in the number of cells obtained from the bone marrow of early life incised or naïve or sham animals isolated at P35 (p=0.617 controls vs. n.inc, ANOVA on Ranks, n=16-18/group). "LPS" indicates LPS+IFNγ stimulation, "si" indicates treatment with

the siRNA against p75NTR, “Combo” indicates both NGF and BDNF stimulation applied. Data shown as mean +/- SEM.

Supplementary Table: Quantification of genes on protein arrays.